European Commission

JRC SCIENCE AND POLICY REPORTS

# Review on engine exhaust sub-23 nm particles

*DRAFT*

B. Giechaskiel, G. Martini
Sustainable Transport Unit
Institute for Energy and Transport


Report EUR xxxxx EN

Joint Research Centre

European Commission
Joint Research Centre
Institute for Energy and Transport

Contact information
Barouch Giechaskiel
Address: Joint Research Centre, Via Enrico Fermi 2749, TP 441, 21027 Ispra (VA), Italy
E-mail: barouch.giechaskiel@jrc.ec.europa.eu
Tel.: +39 0332 78 5312

http://xxxx.jrc.ec.europa.eu/
http://www.jrc.ec.europa.eu/

This publication is a Science and Policy Report by the Joint Research Centre of the European Commission.



JRCxxxxx

EUR xxxxx EN

ISBN xxx-xx-xx-xxxxx-x (PDF)
ISBN xxx-xx-xx-xxxxx-x (print)

ISSN xxxx-xxxx (print)
ISSN xxxx-xxxx (online)

doi:xx.xxxx/xxxxx

Luxembourg: Publications Office of the European Union, 20xx



Printed in Xxxxxx

## Extended summary

The Particle Number (PN) standard was introduced for Diesel Light Duty vehicles in September 2011 (Euro 5b) and is limiting the number of non-volatile particles emitted over the NEDC to $6x10^{11}$ p/km. The new standard effectively necessitated the installation of high-efficient wall-flow DPFs in all diesel vehicles. The same standard will be introduced to gasoline vehicles utilizing direct injection (G-DIs) at Euro 6 stage (September 2014) initially with a limit of $6x10^{12}$ p/km and from September 2017 with $6x10^{11}$ p/km. This 3 year delay was decided in order to allow the manufacturers sufficient time to investigate the possibility of compliance through improvements in the combustion process without the need of Gasoline Particulate Filer (GPF). The PN standard will also be introduced for heavy-duty engines in 2014 (Euro VI).
The PN standard was based on investigations of diesel vehicles and concerns were raised regarding its suitability for gasoline engines. In the current legislation particle number (PN) limits for solid particles >23 nm are prescribed. However it is feared that gasoline engines have smaller particles and thus the current standard cannot capture them. Target of this report was to investigate whether it is necessary and possible to measure <23 nm particles. In other words it was investigated:

1) whether smaller <23 nm solid particles are emitted from engines in considerable concentration focusing on Gasoline Direct Injection (G-DI) engines,
2) whether all volatile particles can be removed efficiently in the PN measurement systems
3) whether any artifacts happen in the PN systems (e.g. formation of non-volatile particles due to pyrolysis), and
4) whether by lowering the lower size the measurement uncertainty increases significantly.

The main conclusions based on a literature survey and experimental investigation at JRC are:

1) Engines emit solid sub-23 nm particles. The average percentage over a cycle (WLTP) is higher for G-DIs (<60%) compared to diesel engines (20%). These percentages are relatively low considering the emission limit levels ($6x10^{11}$ p/km) and the repeatability (10-20%) and reproducibility of the method (50%). These percentages are close to the percentages expected theoretically not to be counted due to the 23 nm cut-off size (5-15%). High emissions can be found when additives are added in the fuel or lubricant.
2) The volatiles are not always removed efficiently in the PN measurement systems. The major issue is re-nucleation of sulfuric acid downstream of the evaporation tube. These particles typically do not grow at sizes above 23 nm.
3) There are indications of formation of 10 nm solid particles from hydrocarbons and sulfuric acid in the PN systems.
4) The measurement uncertainty due to differences between commercial systems will increase. It is estimated to be around 5% for measurements >10 nm, when no separate solid nucleation mode exists.
5) Based on the information today, the PN legislation should remain the same. However investigations should go on measuring <23 nm particles for current and future engines.

The recommendations for proper <23 nm measurements are:

- A catalytic stripper (CS) should be used. It oxidizes the organics of the exhaust gas and traps any sulfur. However, it doesn't necessarily improve on pyrolysis and has higher losses, which will translate into higher measurement variability.
- Without CS the measurements should be conducted with as high as possible primary dilution (PCRF). In case of extreme differences of >23 nm and <23 nm particles, the measurement should be repeated with 10 times higher primary dilution (PCRF).
- Due to extreme losses in the sub-10 nm range and the possibility of artifacts (re-nucleation or pyrolysis) for legislation purposes the measurement of sub-10 nm particles is not recommended.

**Acknowledgments**

The authors would like to thank Dr. M. Maricq and Dr. Athanasios Mamakos for their helpful comments.

## Acronyms

| | |
|---|---|
| APC | AVL Particle Counter |
| ARP | Air Recommended Practice |
| CAST | Combustion Aerosol Standard |
| CMD | Count Median Diameter |
| CS | Catalytic Stripper |
| CVS | Constant Volume Sampling |
| DOC | Diesel Oxidation Catalyst |
| DPF | Diesel Particulate Filter |
| EC/OC | Elemental Carbon / Organic Carbon |
| EEPS | |
| ET | Evaporation Tube |
| G-DI | Gasoline Direct Injection |
| GPF | Gasoline Particulate Filter |
| NEDC | New European Driving Cycle |
| PAH | Poly-aromatic hydrocarbons |
| PCRF | Particle Concentration Reduction Factor |
| PFI | Port Fuel Injection |
| PM | Particulate Matter |
| PMP | Particle Measurement Programme |
| PN | Particle Number |
| PNC | Particle Number Counter |
| RH | Relative Humidity |
| SCR | Selective Catalytic Reduction |
| TEM | Transmission electron microscopy |
| VPR | Volatile Particle Remover |
| WLTP | World Light Duty Testing Procedures |

# Contents

## Introduction

Figure 1 gives a simplified overview of the processes from the combustion in the cylinder of the engine until the sampling point at the full dilution tunnel (CVS). In the combustion chamber primary soot particles (spherules, 10-30 nm) form via the pyrolysis of fuel (and lubricant) molecules when there is not sufficient oxygen for complete oxidation. In this stage fuel (and lubricant) molecules can completely escape combustion and/or be partly modified; however at this stage they remain in the gas phase. The primary particles agglomerate and most of them are oxidized at the high temperatures in the cylinder. As the piston moves downward, the system cools rapidly. At this stage if there are other non-volatile species (like metals) with very high concentrations, they will deposit on the carbon particles or may alternatively self-nucleate.
In the exhaust tailpipe and the transfer tube from the vehicle to the full dilution tunnel the exhaust gas temperature is still high and usually agglomeration goes on. Also previously "stored" material on transfer tube walls can be released. Semi-volatiles such as Polycyclic Aromatic Hydrocarbons (PAHs) can condense on particles. Aggregates have an impure form of near-elemental carbon with a graphite-like structure. The aggregates are typically called soot (or soot carbon). Note however that soot can contain minor amounts of bound heteroelements, especially hydrogen and oxygen.
In the full dilution tunnel the exhaust gas is mixed with room air dilution air. Some volatile material (from unburned fuel and/or lubricant) condenses on the agglomerates and/or creates nucleation mode particles (droplets). Thus at the end of the dilution tunnel there is a tri-modal number distribution (see upper right panel of Figure 1):

- The *nucleation mode*, which contains mainly volatile droplets, but solid cores can also exist
- The *accumulation mode*, which consists mainly of the agglomerates (soot) and the condensed on them volatile material, and
- The *coarse mode*, which consist of deposited particles that reenter in the full dilution tunnel.

Most particles, by mass, reside in the accumulation mode, while by number sometimes the nucleation mode can dominate (Kittelson 1998).
During mixing in the dilution tunnel semi-volatile gaseous species, organics and sulfates partition to the aerosol phase, depending on the local temperature and species concentrations, both of which are a function of dilution ratio (ratio of air to exhaust gas). This partitioning occurs in the form of adsorption and condensation onto existing soot agglomerates or as nucleation of separate particles (droplets), usually between 10-30 nm in diameter. Extensive condensation can change the structure of the agglomerates (Weingartner et al. 1997, Pagels et al 2009). Whether a separate nucleation mode forms, as well as its magnitude, depends on a number of factors. These include the engine characteristics, the aftertreatment devices utilized (Herner et al. 2011, Biswas et al. 2008, Kittelson et al., 2006a, 2006b, Vaaraslahti et al. 2004, Giechaskiel et al. 2005), the pre-conditioning and history of the test (Giechaskiel et al. 2007, Swanson et al. 2009), the fuel and the lubricant used (Kittelson et al. 1978, 2008), the sampling conditions (Khalek et al. 1998, 1999, Mathis et al. 2004a), adsorption phenomena along the sampling lines (Maricq et al. 1999a), and the amount of soot present, since this promotes the competing process of condensation and adsorption instead of nucleation (Khalek et al. 1998,

2000, Vouitsis et al. 2004). In order to avoid the variability of the volatile nucleation mode the European legislation introduced a particle number (PN) method based on the thermal pretreatment of the aerosol and the measurement of the accumulation mode only.

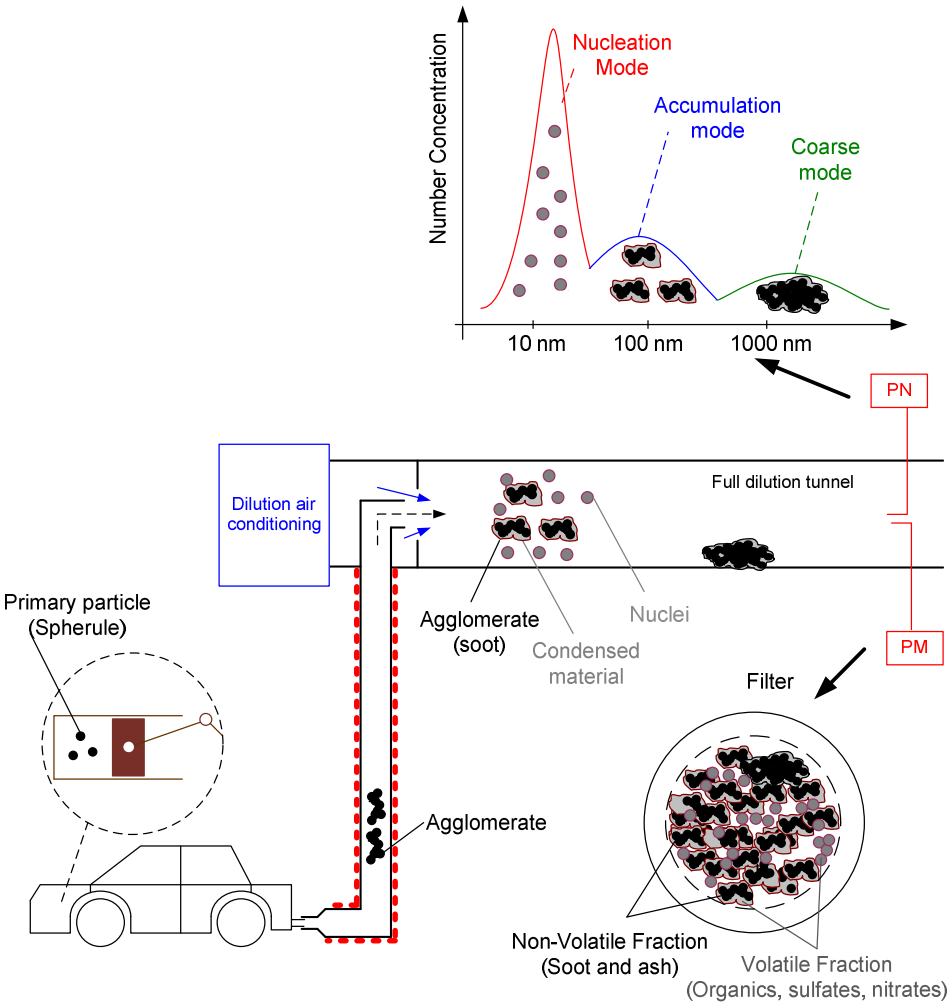


**Figure 1:** *Typical sequence of particle transformation from the engine to the measurement location (from Giechaskiel et al., 2012).*

**Particle Number (PN) method:** The PN method is based on the findings of the Particle Measurement Program (PMP). When the exhaust gas enters the volatile particle remover (VPR) of the particle number system it is heated up to 300-400°C and most volatiles and semi-volatiles evaporate and the particle number distribution is affected (see Figure 2). The particle number counter (PNC) measures particles >23 nm (actually it has a counting efficiency of 50%±12% (cut-off size, $d_{50\%}$) for particles of 23 nm and >90% for 41 nm, so this means that the particle number system measures only the accumulation mode and (depending on whether there is a cyclone or not) the coarse mode. The coarse mode in terms of number doesn't contribute much. Note also that even if the volatiles from the accumulation mode are not completely evaporated the total number concentration is not affected. If the nucleation mode is not completely evaporated, there will be an effect on the number concentration. The 23 nm cut-point of the PNC ensures that this effect will be small. Note however, that if there is a solid nucleation (core) mode, this will not be counted. Details of the legislation requirement for the PN systems can be found in Annex A. In this report, particles after thermal pre-treatment at approximately 350°C are called 'solid'.

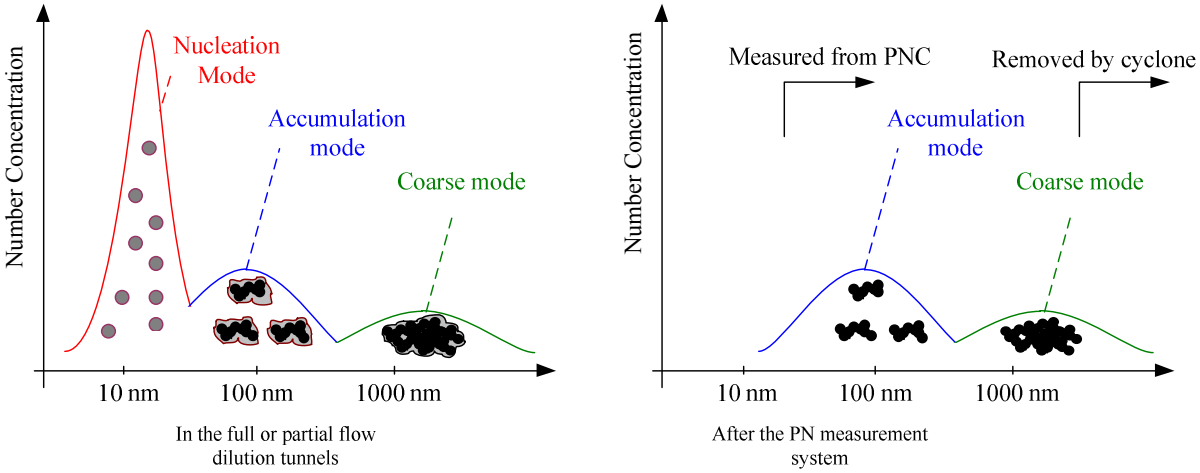


**Figure 2:** *Particle distributions before and after a particle number measurement system.*

Three methods based on the principles of evaporation, adsorption, and oxidation are commonly used to remove volatile components, as shown in Figure 3 (Giechaskiel et al. 2014). Typically temperatures higher than 250°C are required to evaporate volatile particles (Mayer et al., 1998), but in legislation a temperature of 350°C is pre-scribed. Practically, all commercial PN systems use the evaporation tube method.

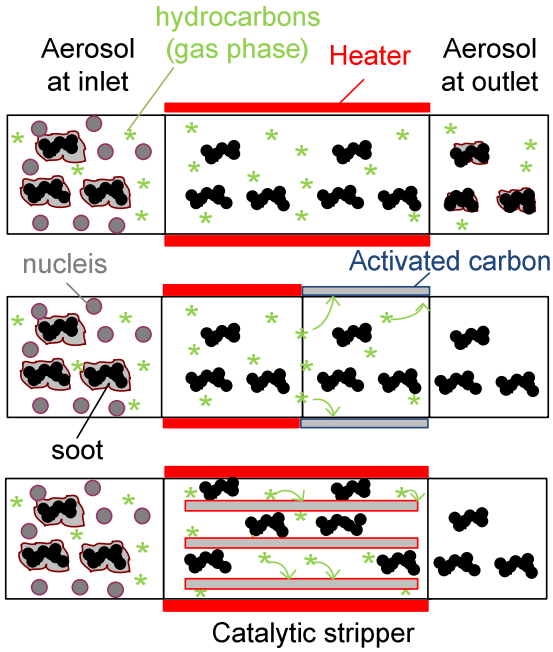


**Figure 3:** *Methods to remove volatile components by a) evaporation, b) adsorption on activated carbon, and c) oxidation by a catalytic stripper.*

The PN standard was introduced for Diesel Light Duty vehicles in September 2011 (Euro 5b) and is limiting the number of non-volatile particles emitted over the NEDC to $6x10^{11}$ p/km. The new standard effectively necessitated the installation of high-efficient wall-flow DPFs in all diesel vehicles. The same standard will be introduced to gasoline vehicles utilizing direct injection (G-DIs) at Euro 6 stage (September 2014) initially with a limit of $6x10^{12}$ p/km and from September 2017 with $6x10^{11}$ p/km. This 3 year delay was decided in order to allow the manufacturers sufficient time to investigate the possibility of compliance through

improvements in the combustion process without the need of Gasoline Particulate Filer (GPF). The PN standard will also be introduced for heavy-duty engines in 2014 (Euro VI).
Note that it is important to distinguish solid particles < 23nm that are part of the lognormal soot accumulation mode from a separate small solid particle mode. Sub 23 nm soot mode particles are already regulated with the current 23nm cut-off size, at least to an extent, even if they are not explicitly counted. For example for typical size distributions with means around 50-70 nm, approximately 5-15% of the total particles are not counted. However, one could theoretically manipulate the size distribution to lower sizes (e.g. mean 30 nm) and thus avoid (e.g. 40%) of the emitted particles to be measured. Lowering the cut-off size reduces these percentages (and the range of these percentages) but at the same time can increase the measurement uncertainty due to different losses in the commercial systems.

Objectives: Target of this report is to investigate whether it is necessary and possible to measure <23 nm particles. In other words it will be investigated 1) whether smaller <23 nm solid particles are emitted by engines in considerable concentration focusing on Gasoline Direct Injection (G-DI) engines, 2) whether all volatile particles can be removed efficiently, 3) whether any artifacts exist (e.g. formation of non-volatile particles due to pyrolysis) and 4) whether a lower than 23 nm size increases significantly the measurement uncertainty. Recommendations for proper <23 nm sampling will be given.

## Health effects

Initially a short overview of the adverse health effects of small particles will be given. Target is to see whether sub-23 nm particles are more harmful than the rest bigger particles.
Particles are emitted from a multitude of sources. The residence time in the atmosphere depends mainly on their size. Owing to the effect of gravity, coarse particles are rapidly removed from the air by sedimentation (residence time between some minutes and some hours); also, particles in the nucleation mode are transformed into coarser particles by coagulation processes. The highest residence time in the atmosphere (up to some weeks) is shown by particles in the accumulation mode, which can be easily transported by the wind up to thousands of kilometers from the area where they are formed. However, it should be kept in mind that in cities people are close to cars and the diluted exhaust gas can reach them in a few seconds/minutes.
Particulates are associated with several environmental problems, like visibility degradation, soiling and damage to materials and global warming. Black carbon, the light-absorbing carbonaceous fraction of PM, is a positive radiative forcing agent and has an established impact on climate change (Menon et al. 2002, Ramanathan and Carmichael 2008), whereas the volatile organic and sulfate components can have positive or negative impacts by altering cloud reflectivity and the size of critical condensation nuclei. Particulates are considered to have a negative impact on the human health. Epidemiological (e.g. Pope 2000) and toxicological studies (e.g. Oberdörster 2000) have associated urban air quality and air pollution, and specifically particulate matter, with adverse health effects. Vehicle exhaust particles have long been considered a significant source of anthropogenically generated particles.
In the most extensive and current review of the literature, EPA (2009) found that for short-term and long-term exposures to Particulate Matter (PM), is still best linked to fine particles, particles whose diameter is less than approximately 2.5 μm. A number of health effect studies suggested that ultrafine particles, particles whose diameter is <100 nm, might be more

hazardous than fine particles (Ferin et al. 1992, Seaton et al. 2009, Manke et al. 2013, Sager and Costranova 2009) but maybe this is not true for all materials (Karlsson et al. 2009). Two are the main reasons for the possibly higher danger of smaller particles: Higher deposition fraction of smaller particles and higher surface area in contact with the human cells (for the same mass).

The three main regions of the respiratory tract are: 1) the extrathoracic region (ET) that consists of the oro- and naso-pharyngeal region and the larynx; (2) the tracheobronchial region (TB), the system of the conductive airways; and 3) the pulmonary region (PU) that contains the fully alveolated alveolar sacs and different types of alveolated airways. Hence, the lung consists of the tracheobronchial (TB) and the pulmonary (PU) regions. The deposition fraction, defined with respect to the inhaled total particle number concentration, is shown in Figure 4 as a function of particle diameter. The deposition fractions in the three characteristic regions of the respiratory tract are presented separately. The deposition location of an inhaled particle is a sensitive function of its diameter since diffusion is the main deposition mechanism, inertial impaction contributing as well, for particles in the size range of emitted diesel-exhaust distributions. The deposition fraction in the ET and TB region is lower for the accumulation mode (particle size around 50-100 nm) but increases for smaller particles. In the PU region the deposition efficiency curve has a maximum around 30 nm but decreases for smaller sizes. Generally the total deposition increases with decreasing size in the region of interest (particles <300 nm).

The deposition location of an inhaled particle is a determining factor in assessing its health effect. Cancers in mouth, larynx, trachea, bronchus and other regions of the lung can be traced to exposure to particles. In the bronchial and bronchiolar airway generations mucociliary clearance eliminates a significant fraction of deposited particles within 24 hours (ICRP 1994). In deeper lung regions the majority of deposited particles remain long enough to interact with lung fluid and epithelial cells. During this interaction mutagen and carcinogen agents such as oxidative radicals are generated (Oberdörster 2000, Brown et al. 2001, Jung et al. 2006). Inflammatory (Salvi et al., 1999b), allergic immune response (Salvi et al., 1999a; Pandya et al., 2002), or cardiovascular consequences (Donaldson & MacNee, 2001) have also been reported.

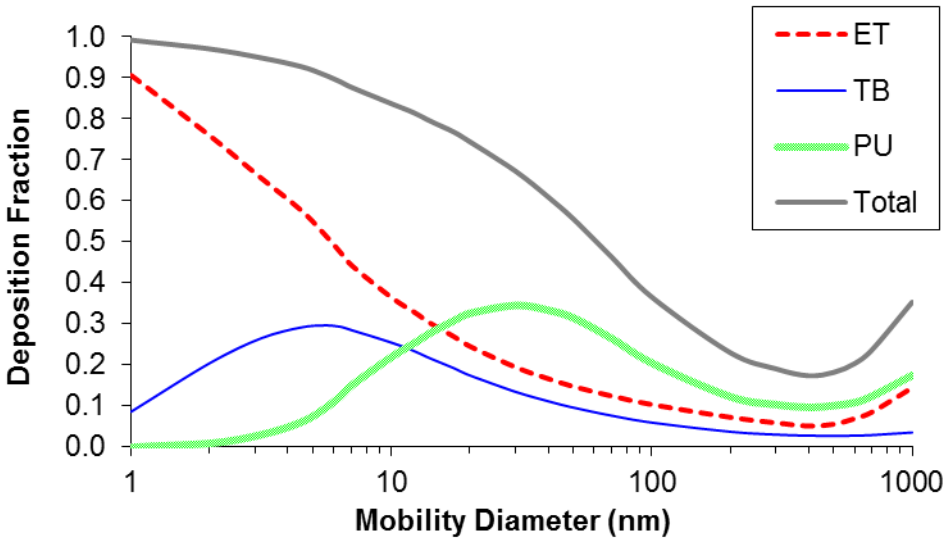


**Figure 4:** *Calculated deposition fraction of inhaled particles as a function of particle diameter for the three region of the human respiratory system: extrathoracic (ET), tracheobronchiolar (TB), and pulmonary (PU). From Alföldy et al. (2009).*

It should also be added that the concept of translocation proposes that inhaled solid nanoparticles pass through the lungs' alveolar membrane and go via the blood to the heart and other organs where they exert a directly toxic effect (Oberdörster et al. 2004). They can cross the blood-brain barrier and can also cross the placenta and enter into the fetus. This doesn't apply for volatile nanoparticles which will dissolve in lipid and aqueous bodily fluids. Pioneering studies (Oberdörster 1996, Donaldson et al. 1998) suggested that the inflammatory response to particles from non-toxic materials correlates better with the particle surface area rather than the mass. Thus it is assumed that nanoparticles are more harmful than bigger particles because they will have larger surface area (for the same mass). Some authors suggest that the soot core is the component that stimulates the most adverse reaction (Gauderman et al. 2004, Mordukhovich et al. 2009, Lovik et al. 1997). Many studies have concluded that the toxicity response of PM primarily depends on its chemical composition (Li et al. 2003, Ntziachristos et al. 2007, Cheung et al. 2009, Cho et al. 2005, Yang et al. 1999, Gojova et al. 2007). Transition metals (like iron, copper, vanadium and zinc) and metal oxides (Jeng and Swanson 2006) also contribute to the oxidative stress resulting from exposure to PM (Geller et al. 2006) and maybe even more than soot (Sager et al. 2009). The high surface activity of metals, which are used in emission control catalysts, seem to increase their adverse health effects (Dick et al. 2003). Moreover, these insoluble nanoparticles can transport other surface adhered toxic substances, a phenomenon that is described as the 'Trojan horse' effect (Limbach et al. 2003).

Conclusions: From the available studies the main conclusions are:

- Total mass still correlates best with adverse health effects. Surface area however seems to be more important (for the same mass).
- Each part of the total mass (soluble and insoluble fraction) has its contribution. Metal oxides also contribute significantly to adverse health effects.
- The size of particles determines the deposition location and deposition fraction. Generally, it increases with decreasing size in the range of particle sizes emitted by vehicles.
- Thus measuring <23 nm solid particles is important if there is high concentration not detected with the current method and/or the nature of this particles is proven to be dangerous for human health.
- This report will focus on the concentration of solid sub-23 nm particles and their nature.

## Primary particles

The $d_{50\%}$ (cut-off size) of the PNC was chosen to be 23 nm in order to include the primary soot particles and at the same time avoid any artifact from volatile nucleation mode particles, which after thermal pretreatment are, if they still exist, <20 nm. This section will examine the first assumption i.e. size of primary particles for different engine categories.
Several studies have investigated the morphology of soot particles from combustion processes using electron microscopy (TEM). Diesel engine soot is composed of agglomerated carbonaceous primary particles (Bérubé et al. 1999, Shi et al. 2000, Kwon et al. 2003, Park et al. 2003, Merola et al. 2003). Solid carbon is formed during combustion in locally fuel-rich regions, and substances such as hydrocarbons can be adsorbed or condensed on the surface of soot particles (Kittelson 1998). The soot particle nanostructure is highly dependent on conditions such as temperature, time, and fuel properties (Wal and Tomasek 2003). The diameter of primary soot particles determined by TEM analysis has been reported to be 22.6±6.0 nm for

diesel soot in a smog chamber (Wentzel et al. 2003). Primary soot particle diameters obtained from TEM analysis have been investigated for light-duty (common-rail, direct-injection) and heavy-duty (single-cylinder, direct-injection) diesel engines (Lee et al. 2001, 2003a, 2003b).The primary soot particle diameter ranged from 19.4 to 32.5 nm for the light-duty engine and from 28.5 to 34.4 nm for the heavy-duty engine. The primary soot particle size decreased with engine load and increased with EGR rate. This behavior was explained by increased soot oxidation due to higher combustion temperature. Similar results were found by Mathis et al. (2005) with sizes ranging from 18 to 32 nm and Neer and Koylu (2007) with sizes between 20 and 35 nm. Similar size of primary particles is believed for gasoline with port fuel injection vehicles (G-PFI) (Kochbach et al. 2005).
Regarding G-DI engines, Mathis et al. (2004b) investigated the volatility of 20 nm particles upon exposure to the TEM electron beam. Significant levels of particle associated sulfur and potassium were measured using energy dispersive x-ray spectrometry. In addition an image of a nanoparticle aggregate with about 27 nm primary particle was shown. Barone et al. (2012) investigated G-DI soot morphology (see Figure 5a). They showed that primary particles were distributed in a range of 7 to 60 nm in diameter, which turned out to be somewhat wider than the size range of diesel particulates (Lee et al. 2002, Lapuerta et al. 2007). For a fuel injection strategy which produced low particle number concentration there were many single solid sub-25 nm particles and fractal like aggregates with primary particle size between 10 and 15 nm. For early fuel injection strategy, liquid droplets were prevalent, and the modal average primary particle diameter was between 20 and 25 nm. Gaddam and Vander Wal (2013) found narrower range (16-23 nm). The TEM morphology examination from Lee et al. (2013) revealed the presence of small nanoparticles, clearly discerned from large aggregate particles. Both nano-sized and large aggregate particles appeared to be agglomeration of nearly-spherical primary particles, where the size of aggregate particles was dependent on the size of primary particles. In the TEM nanostructure examination, particles from gasoline combustion exhibited graphitic structures, regardless of fuel injection timing. However, the nanostructures of 20% ethanol-derived particles were changed to amorphous as the injection timing was advanced. It was finally concluded that those results from SMPS and nanostructure analyses are caused potentially by the increased amount of unburned hydrocarbons or volatile organics due to fuel impingement at that early fuel injection timing (Lee et al. 2013).
TEM images of solid particles <23 nm are rare. Lee et al. (2013) observed 10 nm particles from G-DI engine with carbon-only TEM grids, but not on edges of lacey carbon TEM grids. Mathis et al. (2004b) observed that the 20 nm particles of a G-DI vehicle evaporated within 60 s of exposure to the electron beam. Thus, there are no TEM studies that show a separate solid nucleation mode for G-DI vehicles. For diesel engines solid sub-23 nm particles can be found when additives are added (Lee et al. 2006) (Figure 5b).

Conclusions: The mean value of the primary particles is around 25 nm. No significant differences were observed for G-DI particles. However the following points should be considered for G-DIs: The distribution of particles and primary particles can be wider, so larger percentage of particles can exist <23 nm. The structure of primary particles is sometimes different (more amorphous) probably due to unburned hydrocarbons or volatile organics due to fuel impingement at early fuel injection time. This means that differences in the thermal pre-treatment (temperature, residence time of the PN systems) might lead to different results.

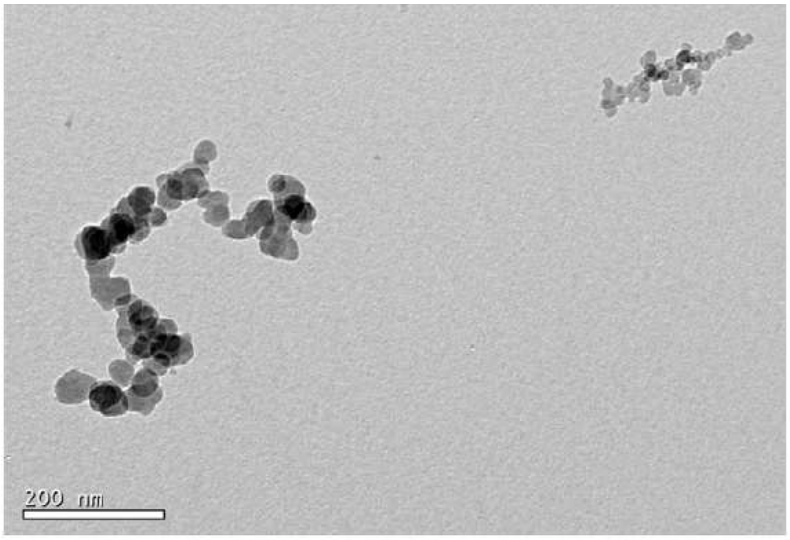


**Figure 5a:** *G-DI nanoparticle aggregates for the condition in which fuel injection timing was modified for low particle number concentration emissions. The average primary particle diameters are 17 and 35 nm for the small and large aggregate, respectively. From Barone et al. (2012).*

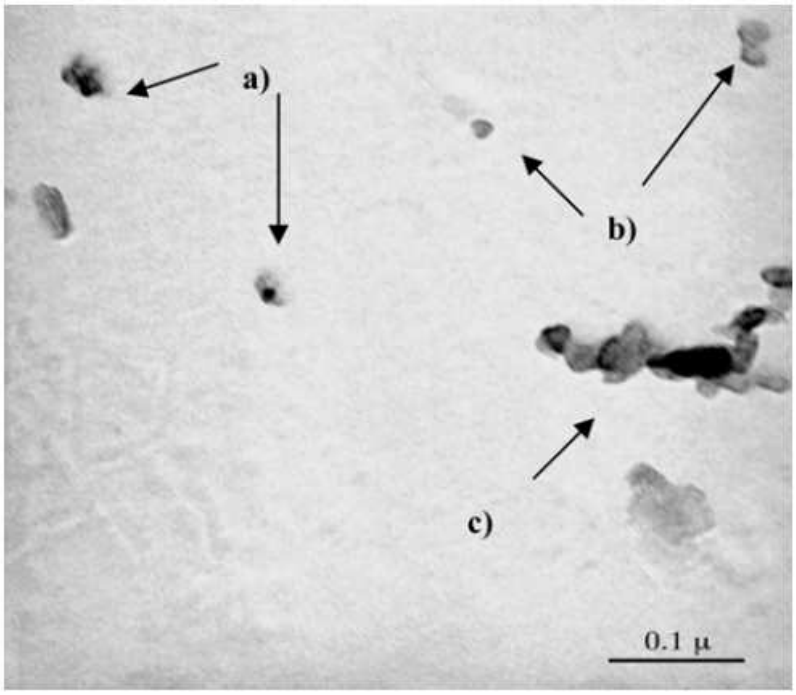


**Figure 5b:** *TEM micrograph of size selected diesel particulate matter (from impactor stage with aerodynamic diameter of 50 nm), showing: (a) nucleated iron particles, (b) hydrocarbon particles, and (c) chain agglomerate particle. Note: 60 ppm iron doping rate. From Lee et al. (2006).*

## Typical size distributions

Table 1 gives typical (solid >23 nm) PN emission ranges of various engine technologies. For this analysis extreme values were not taken into account. The values are based on more than

45 light-duty diesel vehicles without DPF, 35 with DPF, 40 G-DI vehicles and 25 G-PFI vehicles (Karlsson 2005, Zhang et al. 2010, Andersson et al. 2007, Giechaskiel et al. 2008a, Giechaskiel et al. 2008b, Giechaskiel et al. 2010b, 2010c, Mohr et al. 2003a, 2003b, Mohr et al. 2006, Bosteels et al. 2006, May et al. 2008, Maricq et al. 2011, Vogt et al. 2006, 2010, Ntziachristos et al. 2004b, Mamakos et al. 2011a, Mamakos et al. 2011b, Mamakos et al. 2011c, Braisher et al. 2010). The heavy-duty results are based on more than 20 engines without DPF and 10 with DPF. Typical diesel emissions are in the order of $5x10^{13}$ p/km [p/kWh] for both light-duty and heavy-duty and the technology (up to Euro 4 for light-duty and Euro V for heavy-duty) and the fuel has a relatively small effect of <50% (Tzamkiozis et al. 2010). A significant decrease of the emissions (2-3 orders of magnitude) is achieved with the introduction of DPFs.
The G-PFIs are typically below $1x10^{11}$ p/km. However, a recent study by AECC found emissions in excess of $10^{12}$ p/km from a Euro 4 and a Euro 3 G-PFI vehicles having an accumulated mileage of 60000 and 120000 km, respectively, raising some concerns on the potential emission degradation for this vehicle category (May 2011). The G-DIs emit approximately $5x10^{12}$ p/km. Prototype G-DI engines with advanced injection systems and engine calibration (Piock et al. 2011, Whitaker et al. 2011) or commercial G-DIs retrofitted with Gasoline Particulate Filters (GPF) (Saito et al. 2011, Mamakos et al. 2013b) have decreased the PN emissions below the diesel light-duty vehicles PN limit with small fuel consumption penalty.
There are some studies that have examined the (solid) size distributions of light-duty vehicles and heavy-duty engines. Table 1 summarizes the results of more than 15 light-duty diesel vehicles without DPF, 5 with DPF, 10 G-DI vehicles and 30 G-PFI vehicles (Ntziachristos et al. 2004b, Ntziachristos et al. 2005, Giechaskiel et al. 2010c, Khalek et al. 2010, Mamakos et al. 2011a, Mohr et al. 2003a,b, Maricq et al. 1999b, 2002, 2011, Harris and Maricq 2001, Price et al. 2006, Mamakos et al. 2011c, Hall and Dickens 1999, Mohr 2000, Tzamkiozis et al. 2010). The HD results are based on more than 20 engines without DPF and 5 with DPF (Virtanen et al. 2004, Andersson et al. 2001, Thompson et al. 2004, Harris and Maricq 2001, Giechaskiel et al. 2010c, Giechaskiel et al. 2008b). The standard deviations are derived from approximately the 1/3 of the vehicles for which there was information in the texts. The size distributions have count median diameters (CMD) in the range of 50-75 nm (light-duty) and 60-85 nm (heavy-duty) with standard deviations around 1.8-1.9.

**Table 1:** *Typical (solid >23 nm) number emissions PN, count median diameter CMD and standard deviation σ of various engine technologies (assuming lognormal size distributions). Typical PM emissions and chemical composition is also given. HD=Heavy-Duty, LD=Light-Duty.*

| | Technology | PN | CMD | σ | PM | Ash | Soot | Organic | Sulfates |
|---|---|---|---|---|---|---|---|---|---|
| | | [p/km] or [p/kWh] | [nm] | [-] | [mg/km] or [mg/kWh] | [%] | [%] | [%] | [%] |
| HD | Diesel | $5x10^{13}$-$2x10^{14}$ | 50-100 | 1.7-2.1 | 20-80 | 5-10 | 40-75 | 20-50 | 0-15 |
| HD | DPF | $5x10^{10}$-$2x10^{12}$ | 60-75 | 1.6-2.0 | 1-4 | 0-5 | 5-20 | 20-50 | 5-60 |
| LD | Diesel | $2x10^{13}$-$2x10^{14}$ | 40-80 | 1.7-1.9 | 10-40 | 0-5 | 55-90 | 10-40 | 5-15 |
| LD | DPF | $5x10^{10}$-$6x10^{11}$ | 45-75 | 1.7-2.1 | 0-2 | 0-5 | 0-15 | 40-75 | 5-35 |
| LD | G-DI lean | $2x10^{12}$-$2x10^{13}$ | 50-85 | 1.7-2.1 | 1-20 | 0-5 | 55-80 | 20-40 | 0-5 |
| LD | G-DI stoich. | $1x10^{12}$-$8x10^{12}$ | 40-75 | 1.7-2.0 | 1-10 | 0-5 | 75-90 | 10-25 | 0-5 |
| LD | G-PFI | $2x10^{10}$-$6x10^{11}$ | 45-75 | 1.6-2.2 | 0-2 | 0-5 | 10-25 | 45-80 | 10-40 |

Conclusions: The PMP legislation was based on typical engine exhaust size distributions with means of 40-70 nm and standard deviation of 1.7-1.9. It was also observed that DPFs trap almost equally all particle sizes.

## Solid <23 nm particles (literature survey)

Although it was believed that there were no solid particles <23 nm (except when additives were present), the last years many studies showed that this is not the case. Table C1 in the Annex B summarizes the studies that have found solid particles <23 nm. Only the studies with thermal pre-treatment were considered. Some studies with lower temperatures than 250°C were included in grey. Studies without any thermal pre-treatment that typically favor the volatile nucleation mode formation were not considered at all. The main conclusions are summarized below.

### Diesel (40 engines and vehicles)

A solid nucleation mode has been measured with older (Kittelson et al. 2006a) and modern diesel engines without exhaust aftertreatment (Rönkkö et al. 2007) or with low particle collection efficiency filters (Heikkilä et al. 2009) and/or DOCs (De Filippo and Maricq 2008, Lähde et al. 2009, 2010). It appears mostly at idle and low loads (De Filippo and Maricq 2008, Mayer et al. 2010) but even at high (Lähde et al. 2009). It becomes more prominent when the EGR is forced low. The solid nucleation mode increases along with NO and overall $NO_x$ emissions, in contrast with the accumulation mode (Lähde et al. 2010). The solid core could consist of soot, metal oxides or low volatility organic compounds (Sakurai et al. 2003, Kittelson et al. 2005, 2006a, Rönkkö et al. 2007). The nature of these particles will be discussed below.

*Low volatility components:* Chemical analysis of nucleation mode particles of a heavy-duty engine showed that although organic carbon was the primary component (79%) elemental carbon (8%), elements (4%) and ions (9%) existed as well (Fushimi et al. 2011). The authors also found that lubricating oil was the primary component of the nuclei particles.

*Metal oxides (lubricant):* Elements such as S, Ca, Zn and P have been found in high concentrations (Fushimi et al. 2011). These elements are used as antioxidants (e.g. ZnDTP) and detergent-dispersants (e.g. $CaCO_3$). The assumption is that metal particles from the lubricant are partially vaporized during combustion and nucleate. Metals from the coatings of catalytic converters and particulate filters (e.g. Pt, Va) are assumed to be low (ng/km) and in the μm range. Similarly for abrasion metals (e.g. Fe, Cr, Ni, Cu, Pb) from piston rings, valves and bearings. They will probably be washed away by the oil film and may end up in the lubrication oil sump or oil filter, however it cannot be excluded that they can re-entrain in the combustion chamber and thus be vaporized and form solid nucleation mode particles (Mayer et al. 2010). Emissions can reach 1 mg/km (or 1 mg/kWh) (Mayer et al. 2010). High solid nucleation mode is found when the soot mode is low and at idle. The lube oil consumption is high in this case because the engine blow-by gas flow from cylinder to oil sump, which usually pushes back the lubrication film, is weak. Thus more lubrication oil intrude in the combustion (Mayer et al. 2010).

*Metal oxides (fuel):* Fuel additives (fuel borne catalysts, like Fe and Ce) can also result in a solid nucleation mode (Jung et al. 2005). These are added in small concentrations to promote regeneration in DPFs. At low concentrations no solid nucleation peak is observed (Burtscher et al. 1998, Skillas et al. 2000). The additives are deposited on larger soot particles to catalyze the soot combustion. Overdosing the additives (fuel born catalyst) results in a separate solid nucleation peak (Mayer et al. 2010) due to self-nucleation and reduced soot surface for condensation (Lim et al. 2009).

*Soot:* Another assumption is that the solid nucleation mode consists of soot-like particles. In light-duty diesel TEM images were unsuccessful and only by defocusing the TEM could faint roughly 10 nm smudges be seen (De Filippo and Maricq 2008). The explanation was that these solid nucleis were amorphous and couldn't be distinguished from the carbon substrate. The lack of a clear TEM image, their low volatility and the charge distribution rule out that these particles derive from ash or sulfate and suggest rather that they have composition similar to the incipient soot mode observed at <10 nm in rich flames (Sgro et al. 2011, Maricq 2012), or derive from heavy hydrocarbons that nucleate already in the engine cylinder (De Filippo and Maricq 2008, Lähde et al. 2009). How the two solid particle modes (nucleation and accumulation) can originate during diesel combustion is currently not known. Possibly the multiple fuel injection pulses per engine cycle used in new engine technology diesel engines to control soot formation and noise can produce separate particle populations (De Filippo and Maricq 2008). It should be also mentioned that most of these studies that found a soot-like solid nucleation were conducted with thermodenuders which have been found to form artifacts at small particle sizes (see section Thermodenuders).

An important finding was that DPFs remove the solid nucleis with an efficiency comparable to soot. However, regeneration can also result in increased emissions of sub-23 nm solid particles (Clauda et al. 2006). It is suggested that they originate from the fragmentation of the soot cake of the DPF. However, they could also be released metal oxide particles previously adhered to soot particles (Mayer et al. 2010).
It should be mentioned that in many studies it was recognized that the 'solid' nucleation mode was actually volatile, thus an artifact of the PMP method and the dilution factors employed (e.g. Mamakos et al. 2013a, Zheng et al. 2012). This will be topic of later sections.

### G-PFI (8 vehicles)

Solid nucleation mode is often observed and it is assumed to originate from the metals of the lube oil (Mayer et al. 2012). Big differences can be found between old and new engines. A solid nucleation mode has been observed when fuel additives were used (Gidney et al. 2010). The fuel additives were Mn, Fe and Pb in concentrations up to 18 ppm. Very high metal oxide emissions at a size of 10 nm were measured. This case is still realistic in some countries.

### G-DI (10 engines and vehicles)

A shoulder at 20 nm appears quite often (Szybist et al. 2011, Johansson et al. 2013). A separate solid nucleation mode is not typical, but the size distribution can peak at small sizes (20 nm or lower) in some engine operation modes (Maricq et al. 1999b, Hedge et al. 2011) with EGR and high speed. Fuel with 85% ethanol has also been shown to result in small particle sizes (Szybist et al. 2011).

### Moped (12 mopeds)

Very often the size distribution after thermal pre-treatment peaks at or below 20 nm (Mayer et al. 2012, Czerwinski et al. 2013). Although in some cases it can be a sampling artifact (Giechaskiel et al. 2010c), probably they are particles remaining from the lube oil. The 2-stroke engines are lubricated by adding 2% of lubrication oil to the fuel. The specific fuel consumption is also high. Thus the metal oxide emissions are typically much higher than the 4-stroke engines. With a 2% lubricant addition in the fuel more than 2000 ppm of metals are added.

Metal free lubrication oils reduce the emissions. Low levels of black carbon have also been measured suggesting also soot nucleis (Giechskiel et al. 2010c).

Conclusions: Recent studies, in contrast to older studies, showed that there are particles <23 nm and they could appear in significant concentrations. These particles are considered to be either metals from the lubricant, additives in the fuel or soot particles (heavy molecular hydrocarbons) formed in the combustion chamber. Thus cases with fuel or lubricant (metal) additives or high lubricant consumption need special attention.

## Experimental investigation at JRC (Solids <23 nm)

During September – November 2013 the existence of solid sub-23 nm particles was investigated at the Joint Research Center in Ispra, Italy. A TSI PNC 3025A ($d_{50\%}$=3 nm) was connected in parallel with a TSI PNC 3790 ($d_{50\%}$=23 nm) in a PMP system (AVL Particle Counter, APC) connected to the CVS (Giechaskiel et al. 2010d). The Particle number Concentration Reduction Factor (PCRF) was always 1000 (100x10) for all vehicles examined (see section 'Penetration (losses in the VPR)' for more explanations for the PCRF). The results of WLTP cycles can be seen in Figure 5. Figure 6 gives some examples of size distributions. These were measured with an Engine Exhaust Particle Sizer (EEPS) from TSI connected to a PMP system (APC from AVL) connected to the tailpipe. The PCRF was 15x15.
The following conclusions can be drawn:

- G-DIs have slightly higher percentage of solid sub-23 nm particles compared to diesel vehicles. Diesel vehicles are on the 20% range, while G-DIs on the <60% range.
- Size distribution measurements showed sometimes a solid nucleation mode peaking approximately at 10 nm, usually as a small shoulder, but rarely as a separate nucleation mode. It should be mentioned that this nucleation mode could be a result of the not accurate algorithm of the EEPS to convert current to number concentration for aggregates (EEPS counts based on electrical charge of particles and not by optical detection like the PNCs). This could also be the reason of wider size distribution for G-DI vehicles. Note also that the losses in the VPR in the 10 nm range can be more than 50%, thus the concentration could be higher.
- No extreme percentages were observed at the $10^{12}$ p/km range (and higher).
- The percentage seems to increase at lower emission levels (<$10^{11}$ p/km). However, this could be due to the lower concentrations measured with the 3025A (which uses internal averaging)
- Low ambient temperatures (-7°C) increase this percentage.
- Size distribution measurements during the regeneration and after the regeneration from one vehicle revealed that there were no solid particles <23 nm. One case with high emissions during regeneration was due to re-nucleation after the evaporation tube (see Section 'Experimental investigation at JRC (artifact <23 nm)').
- Tests with mopeds also revealed that volatiles can be measured as solids (<23 nm) (see Section 'Experimental investigation at JRC (artifact <23 nm)').

These tests didn't include heavy-duty engines, which were shown to form solid nucleation mode very often. This needs to be further investigated.

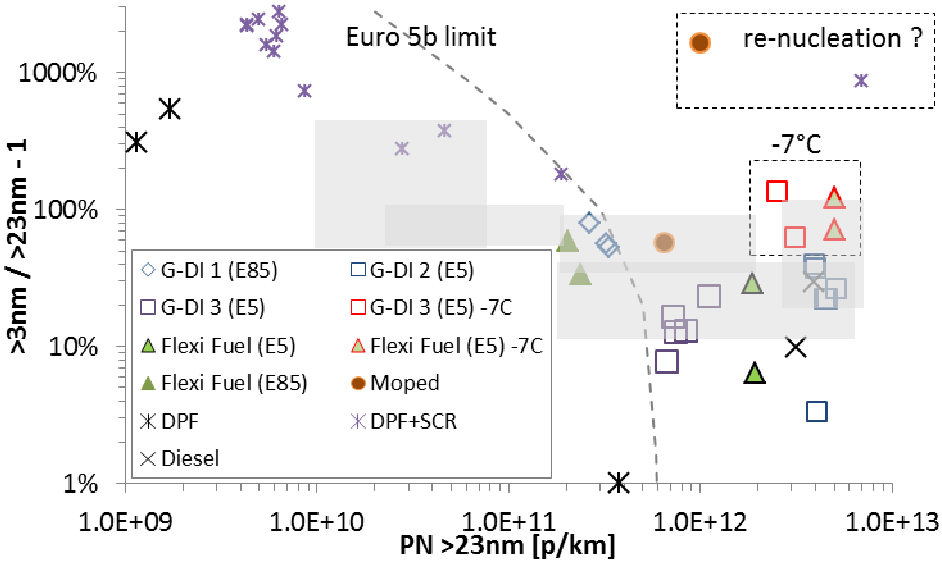


**Figure 5:** *Sub-23 nm particles in function of the solid >23 nm PN emissions (WLTP cycles). Grey areas are ranges reported in the literature for various cycles. The Euro 5b limit refers to the NEDC type approval cycle.*

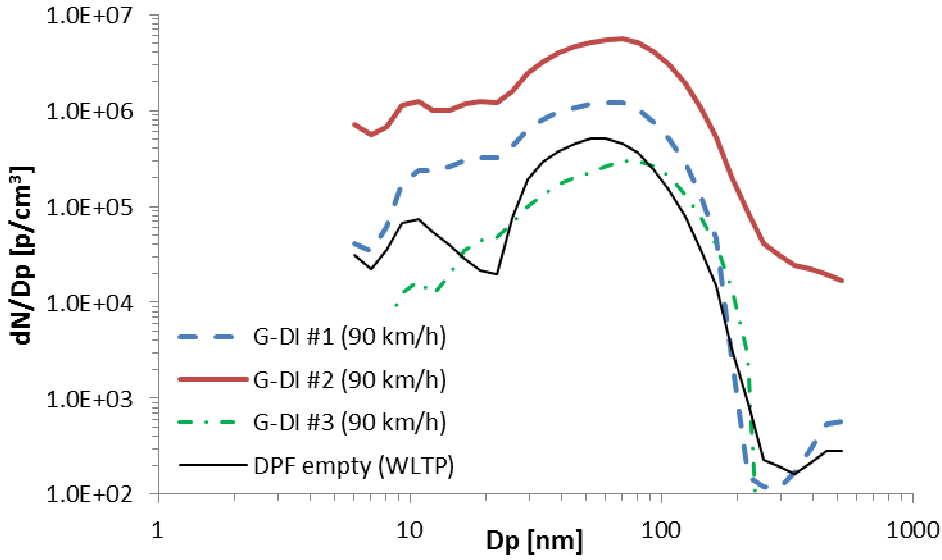


**Figure 6:** *Examples of size distributions measured with G-DI and DPF vehicles. EEPS (from TSI) was measuring downstream of a VPR (APC from AVL) connected to the tailpipe. Size distributions not corrected for losses in the VPR.*

Conclusions: The conclusion is that for emission levels around $10^{12}$ p/km, the percentage of particles <23 nm is around 20% for Diesel vehicles and 30-60% for G-DIs. Thus, at emission levels at the current limit ($6x10^{11}$ p/km), the inclusion of sub-23 nm particles does not lead to exceedance of the limit, although a potential shift to lower size might require adjustment of the limit (see section 'Penetration'). Size distribution measurements showed sometimes a small shoulder peaking approximately at 10 nm; however it could be due to the principle of the operation of the instrument used (EEPS).

## Feasibility of sub 23 nm measurement for PNCs

The cut-off size ($d_{50\%}$) of a PN system is mainly determined by the PNC. Using a PNC with lower than 23 nm cut-off size is possible. Various full flow (no internal splitting or dilution) models exist in the market with cut-off sizes down to 5 nm.

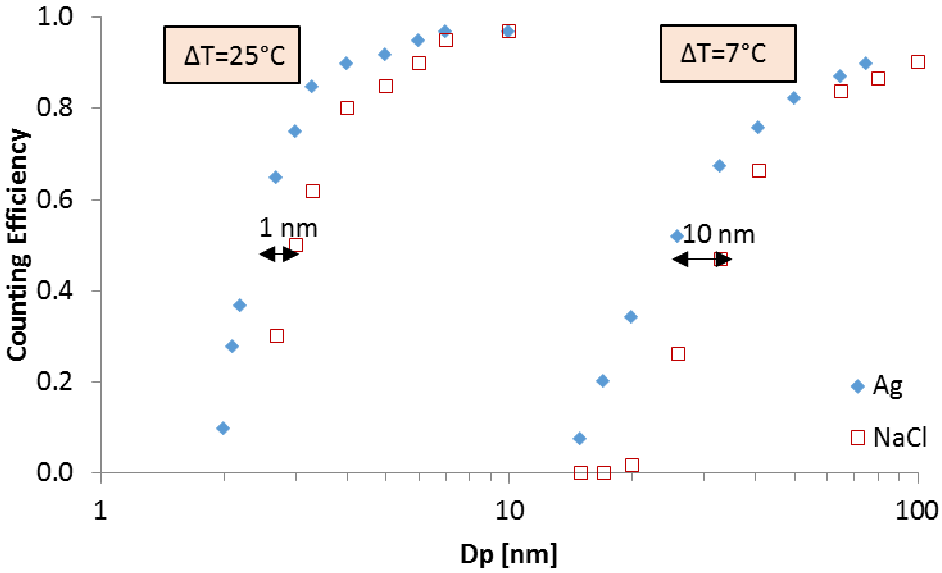


**Figure 7:** *Counting efficiencies of PNCs with different temperature differences between saturator and condenser (from Wang et al. 2010 and Kesten et al. 1991).*

The cut-off size of the low temperature difference PMP PNCs (ΔT=7.5°C) depends strongly on the particle material (e.g. structure, surface properties etc.) (Giechaskiel et al. 2009b, Wang et al. 2010, Giechaskiel et al. 2011). For example, the $d_{50\%}$ for emery oil and NaCl have a difference of 12.5 nm and the difference between oxidized Ag and NaCl $d_{50\%}$ is around 9 nm (Wang et al. 2010). However, for high ΔT (lower cut-off) smaller differences are noticed (in absolute values); note however that in relative terms the effect is quite similar. For example, Kesten et al. (1991) found only 0.7 nm difference between the Ag and NaCl cut-off diameters, for a PNC 3025 with ΔT=25°C. Hermann et al. (2007) who measured different TSI models found smaller effect of the material (Ag and NaCl in this case) with decreasing $d_{50\%}$. Figure 7 shows an example the effect of the material (Ag and NaCl) on the counting efficiencies of two PNCs with different temperature difference between the saturator and the condenser.
One point that needs attention is the calibration material. The most commonly used aerosol for automotive PNCs (emery oil) can be used for 10 nm, but not for 5 nm because it's extremely difficult to produce high concentration at such low size. NaCl and spark soot is difficult to be used because the concentration at these sizes is very low. Materials that can be used are Ag and soot from diffusion flame (e.g. CAST generator). The mini CAST that can produce size distributions with means down to 7-10 nm has to be investigated, because the properties of such small soot particles are not known.
The second point is the verification of the PNCs. While in the current legislation validation (or even calibration) is allowed with another reference PNC, if the lower size is reduced to 5 nm then the possibilities for a reference PNC with even lower cut-off size are reduced. Thus the electrometer will probably be the only reference instrument allowed.

Conclusions: Lowering the cut-off size is feasible and probably advantageous (less dependence on particles' material) for the calibration and the actual emission measurements. The cut-off size of existing systems can change (permanently or interchangeably) down to 10 nm relatively easily without high investment costs. Lower than 10 nm cut-off sizes need different designs of PNCs that do not necessarily fit in the existing VPRs. For lower than 10 nm PNCs, the calibration material has to be re-investigated if the cut-off size will be reduced, because it's not so easy to produce small emery oil particles at high enough concentrations.

## Feasibility of sub 23 nm measurement for VPRs

This section will examine the issues for VPRs if the lower detectable size will be decreased; more specifically the losses in the VPRs (penetrations), formation of particles in the VPR (e.g. pyrolysis) and the volatile removal efficiency of the VPR.

### Penetration (losses in the VPR)

Ideally a VPR should have no particle losses. In this case the measured concentration is determined only by the PNC counting efficiency. However due to diffusion all VPRs have losses that increase with decreasing particle size. Different diffusion and thermophoressis losses also result in different penetrations between different systems. Typical penetration curves of VPRs are shown in Figure 8. Two of them are based on the minimum *requirements* of the World Harmonized Light Duty Procedures (WLTP) and the Air Recommended Practice (ARP) for sampling exhaust gas of aircraft turbines. A curve shows a typical curve for commercial VPRs with evaporation tubes (ET) in the market. The fourth curve is based on a prototype system. The prototype was the VPR that was used for the Round Robin exercise for the determination of the calibration procedures of the VPRs. Approximately 10% losses were found down to 30 nm (Mamakos et al. 2012) and diffusion losses were added for a case of a tube with 3 s residence time as allowed in the current legislation.
Figure 8 shows also the penetrations for particles of <23 nm. It can be seen that the losses increase rapidly. Penetrations of 10 nm particles at the VPRs are between 15% and 40%, but could be 70% at prototype systems. These results indicate that measurements below 10 nm are difficult and will have high uncertainty, because high correction factors are needed. The size distributions of Figure 6 were measured from a PMP system with penetration between the PMP-ET and PMP curves of Figure 8. Nevertheless, the solid nucleation mode could be measured. However the absolute level is not known and a correction factor of >2 would probably be necessary for the sub 23 nm.
In order to take into account these losses legislation corrects the PNC measurements with a mean Particle Number Concentration Reduction Factor (PCRF). This mean PCRF is determined by calibration of the VPRs with monodisperse solid particles of 30, 50 and 100 nm and concentration >5000 p/cm$^3$. The ratios of 30 nm and 50 nm particles PCRFs have to be <1.3 and 1.2 times the 100 nm PCRF. Table 2 shows what a system reports compared to the true inlet concentration for different cases (detailed explanation in Annex C):

- *PMP-1:* PNC with $d_{50\%}$ at 23 nm and VPR with ratio 1.30 (30 to 100 nm) and 1.12 (50 to 100 nm). The 15 nm to 100 nm ratio is 2.21. The mean PCRF is calculated from the 30, 50 and 100 nm PCRFs.

- *PMP-2:* PNC with $d_{50\%}$ at 23 nm and VPR with ratio 1.28 (30 to 100 nm) and 1.09 (50 to 100 nm). In this case the 15 to 100 nm ratio is 1.55. The mean PCRF is calculated from the 30, 50 and 100 nm PCRFs.
- *ARP-1:* PNC with $d_{50\%}$ at 10 nm and VPR with ratio 1.30 (30 to 100 nm) and 1.12 (50 to 100 nm). The 15 nm to 100 nm ratio is 2.21. The mean PCRF is calculated from the 30, 50 and 100 nm PCRFs.
- *ARP-2:* PNC with $d_{50\%}$ at 10 nm and VPR with ratio 1.28 (30 to 100 nm) and 1.09 (50 to 100 nm). In this case the 15 to 100 nm ratio is 1.55. The mean PCRF is calculated from the 30, 50 and 100 nm PCRFs.
- *ARP-4x:* PNC with $d_{50\%}$ at 10 nm and VPR with ratio 1.30 (30 to 100 nm) and 1.12 (50 to 100 nm). The 15 nm to 100 nm ratio is 2.21. The mean PCRF is calculated from the 15, 30, 50 and 100 nm PCRFs.

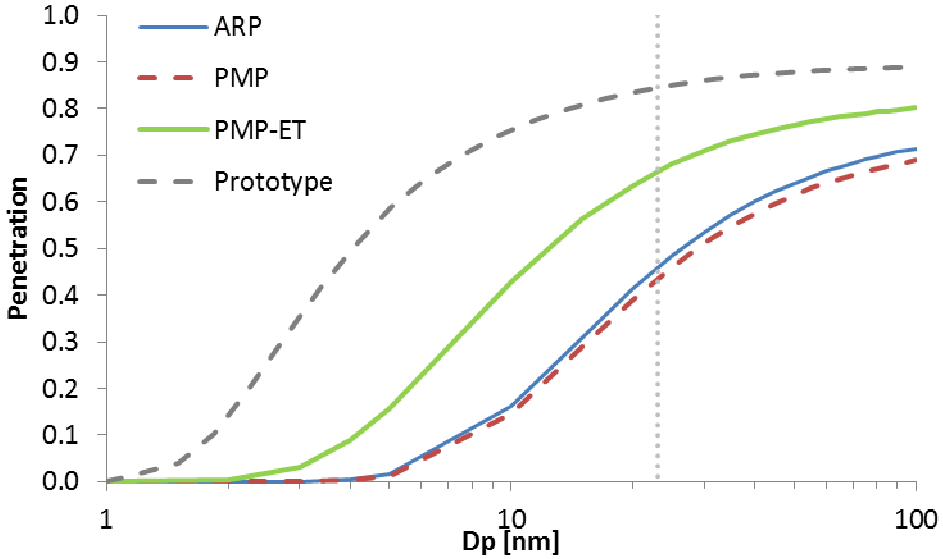


**Figure 8:** *Typical penetration curves of VPRs and minimum requirements based on PMP/WLTP and ARP.*

PMP-1 and PMP-2 are systems with different VPR penetration curves. ARP-1 and ARP-2 are the two PMP systems with PNCs at 10 nm instead of 23 nm. PMP-4x is the PMP-1 system using the PCRF of 15, 30, 50 and 100 nm (extra 15 nm).
As it can be seen in Table 2, this mean PCRF correction generally slightly (5-10%) underestimates the 'true' upstream emissions for typical vehicle size distributions with Count Median Diameter (CMD) between 50 and 70 nm but can slightly overestimate for bigger sizes (see PMP-1 and PMP-2 columns for 50-90 nm mean sizes). However, when the CMD of the size distributions is <50 nm, the final result can be much lower compared to the actual PN concentration entering the VPR. Furthermore, different PN systems can exhibit around 5% differences in the PN results, even if they comply with the legislation requirements, due to the different VPR penetrations (compare PMP-1 and PMP-2 percentages).
Considering the ARP cases it can be observed:

- Higher percentage of the size distribution is measured, thus the above mentioned percentages increase
- For means 50-90 nm, the measured emissions are within -2% and +5% of the true (inlet) emissions

- The difference between different commercial systems should remain around 5%
- For means <50 nm higher percentage of the inlet distribution is measured (compared to the PMP systems). However, this results in higher differences between the commercial systems and thus measurement variability (reproducibility).

If a lower cut-off size will be included in the legislation the main question that arises is whether the mean PCRF should also include a lower size. It can be observed from Table 2 that the mean PCRF that includes the 15 nm results in >50% overestimation of the true PN emissions, assuming that the typical size distribution remain between 50 and 90 nm (see column PMP-4x). Thus, even when the lower cut-off size is reduced the mean PCRF determination should remain the same (i.e. it should be determined only at 30, 50 and 100 nm). This would also help keeping the link to the past measurements. A requirement for e.g. the 15 nm PCRF compared to the PCRF of 100 nm should be added nevertheless to ensure systems with minimum losses.

One other issue with the introduction of lower sizes is the aerosol that can be used for the calibration of the VPRs. Most generators (NaCl and spark soot) cannot produce so low sizes. Silver generators could be used, but with these generators it's not possible to generate bigger particles (e.g. 100 nm). The only generator that could be used for such wide range is the mini CAST generator. The thermal stability of the small nanoparticles however has to be ensured. It should be also realized that such small particles do not necessarily have the same properties as soot but are more PAH like due to the short residence time in the flame.

**Table 2:** *Ratio of final PN result compared to the PN concentration at the inlet of the PN system for different inlet size distributions and PNC counting efficiencies $CE_i$ and VPR Particle Number Concentration Reduction Factor $PCRF_i$ ratios at size i.*

| | **Case** | **PMP-1** | **PMP-2** | **ARP-1** | **ARP-2** | **PMP-4x** |
|---|---|---|---|---|---|---|
| **PNC** | $CE_{50\%}$ | 23 nm | 23 nm | 10 nm | 10 nm | 10 nm |
| | $CE_{90\%1}$ | 41 nm | 41 nm | 15 nm | 15 nm | 41 nm |
| | slope | 1.00 | 1.00 | 1.00 | 1.00 | 1.00 |
| **VPR** | $PCRF_{15}$ | - (2.21) | - (1.55) | - (2.21) | - (1.55) | 2.21 |
| | $PCRF_{30}$ | 1.30 | 1.28 | 1.30 | 1.28 | 1.30 |
| | $PCRF_{50}$ | 1.12 | 1.09 | 1.12 | 1.09 | 1.12 |
| **CMD** | **σ** | **Final PN concentration compared to inlet concentration** | | | | |
| 10 nm | 1.3 | 0% | 1% | 18% | 35% | 30% |
| 20 nm | 1.4 | 29% | 34% | 64% | 82% | 105% |
| 30 nm | 1.6 | 61% | 64% | 83% | 91% | 135% |
| 40 nm | 1.7 | 78% | 79% | 92% | 96% | 151% |
| 50 nm | 1.8 | 88% | 86% | 98% | 98% | 160% |
| 70 nm | 1.9 | 100% | 95% | 105% | 101% | 172% |
| 90 nm | 2.0 | 105% | 98% | 109% | 102% | 178% |
| 10 nm (50%) + 50 nm (50%) | 1.3 + 1.8 | 44% | 44% | 58% | 67% | 95% |

Conclusions:

- The losses of VPRs increase significantly at low sizes (<23 nm). Measurements down to approximately 10 nm are feasible only as indication of existence of particles (the accurate quantification is extremely difficult). Even in that case the PCRF determination should be with monodisperse particles of 30, 50 and 100 nm.

- By lowering the cut-off size, the measurement uncertainty due to differences in the penetrations of commercial systems will not be affected for typical size distributions (between 50 and 90 nm). However, for smaller than 50 nm means, the uncertainty is expected to increase, due to the differences of the penetration curves of the commercial systems.
- It is difficult to generate solid particles <30 nm for the VPR calibration with the most commonly used generators (NaCl, Spark, CAST) but not impossible (e.g. mini-CAST).

## Formation of particles in the VPR

Some researchers (Swanson and Kittelson, 2010, Zheng et al. 2011) have suggested pyrolysis and/or charring of semi-volatiles in the evaporation tube or the thermodenuder. This may actually lead to the formation of a solid nucleation mode artifact, i.e. hydrocarbons will be counted as solid particles. The mechanism of this type of solid formation is not yet clear. It is known that n-alkanes, such as tetracosane and tetracontane, do not react well with sulfuric acid in gas phase (Burwell et al. 1954). However, Swanson and Kittelson (2010) have proposed such reactions to explain this type of solid particle formation. The pyrolysis or charring of organic carbon that occurs during elemental carbon/organic carbon (EC/OC) analysis depends on many factors, especially temperature, but also composition and amount (Yu et al. 2002). Alternatively, dehydration may be occurring where the sulfuric acid is removing hydrogens from the organic carbon, leaving just solid carbon that is measured in the particle phase. In this case, an analogous reaction is the well-known reaction of sucrose with strong sulfuric acid (Shakhashiri, 1983). Another hypothesis is that n-alkanes are oxidized on the hot metal tube walls heterogeneously and then reacted with sulfuric acid to produce a non-volatile salt (Zheng et al. 2011). The explanation that sulfate is a precursor to solid particles is supported by the fact that experiments with pure hydrocarbon particles showed no solid particles and that formation of solid particles was only observed in the thermodenuder and not the catalytic stripper (CS). The sulfur trap in the CS removes the sulfuric acid precursors that may be required for the solid particles to form. Additionally, the CS and thermodenuder both operate at 300°C (wall temperature) but the details of the heating magnitude and duration may influence the result in ways that we do not yet understand. Further, it is not fully clear if the formation of solid particles depends on the size or concentration of semi-volatile particles or if solid particles formed at very low challenge aerosol concentrations and were not detected due to high losses in the system and instrument sensitivity at 5nm. More studies are needed to thoroughly understand the mechanism of particle formation in the heated tubes.

## Volatile Removal efficiency of the VPR

European legislation requires the measurement of solid particles in order to avoid the uncertainties that measurements of volatile particles have. Evaporation is used by European regulations to remove volatiles before the measurement of solid PN concentration. Hot dilution at 10:1 and 150°C followed by an evaporation tube at 350°C are prescribed. The volatile removal efficiency is checked at the lowest dilution setting with tetracontane particles of >30 nm particles and concentration $>10^4$ p/cm$^3$. The volatile removal efficiency should be >99%. The following sections will described the following topics:

- Theoretical volatile removal efficiency of an evaporation tube (incomplete evaporation)
- Re-nucleation after an evaporation tube

Then the other two methods for the removal of volatiles will be described: thermodenuder and catalytic stripper.

### Evaporation tube (ET)

**1) Evaporation:** The residence time and the volatile particle concentration affect the removal efficiency. This method should be used downstream of a dilutor to avoid supersaturation and re-nucleation as the aerosol exits the evaporation tube and cools (Giechaskiel and Drossinos, 2010). Experiments showed that 30 nm heavy alkane (tetracontane) particles can be removed with >99% efficiency in a heated tube with aerosol temperature >200°C, with decreasing efficiency for larger particles (Giechaskiel and Drossinos, 2010). The evaporation is extremely fast (ms) thus the residence time in most evaporation tubes (>0.2 s) in enough. Experimentally it was shown that mass of 0.1 mg/m$^3$ tetracontane could be removed (Giechaskiel and Drossinos 2010) or even higher (Giechaskiel et al. 2009c) for various PMP systems. Limited number of tests at different evaporation tube temperatures (300°C and 500°C) with real exhaust aerosol haven't shown any difference in the results of PNCs with $d_{50\%}$ at 11 nm indicating that the incomplete evaporation of the nucleation mode is not likely for diesel vehicles (Zheng et al. 2012).

**2) Re-nucleation of hydrocarbons:** It was estimated that homogeneous nucleation of evaporated hydrocarbons (tetracontane) vapor at the tube exit would only occur at extremely high concentrations of 30 nm particles (>$10^7$ p/cm$^3$ or 3 mg/m$^3$). At lower concentrations, some condensation may occur onto the solid particles, but this will not affect the solid PN concentration. A diesel vehicle without an oxidation catalyst could emit concentrations of organics up to 70 mg/m$^3$ (e.g., Giechaskiel et al. 2007a) although usually much lower concentrations are measured (e.g., 5 mg/m$^3$ in Ng et al. 2007). Lower volatile emissions are expected for diesel engines with oxidation catalyst (<1 mg/m$^3$) but can be much higher at higher speeds probably due to desorption of volatile material form the exhaust pipe walls (>4 mg/m$^3$) (Giechaskiel et al. 2009c).
During regeneration of Diesel Particulate Filters (DPF) high emissions of nucleation mode particles are observed. Hydrocarbons and sulfur compounds from fuel and lube oil that accumulate in the soot layer in a DPF are released during the high regeneration temperatures. Full dilution tunnel (CVS) measurements of the emitted number distribution during regeneration showed that the mean nucleation mode diameter can be up to 40 nm (Giechaskiel et al. 2007b). Estimates of the mass concentration of nucleation mode particles (assuming a density of 1 g/cm$^3$) give >5 mg/m$^3$.
The maximum value of 70 mg/m$^3$ translates to a maximum mass concentration of 1.5 mg/m$^3$ entering the evaporation tube (considering a dilution ratio of 5 at the full dilution tunnel and 10 at the primary diluter). This mass concentration is lower than the necessary for re-nucleation.
However mopeds have much higher emissions of organics that can reach 700 mg/m$^3$ (Giechaskiel et al. 2010c). This translates to >10 mg/m$^3$ at the outlet of the evaporation tube. Such a high concentration can result in re-nucleation.

**3) Re-nucleation of sulfuric acid:** Since $H_2SO_4$ nucleates easier in the presence of $H_2O$, an empirical equation can be used to determine the critical concentration $C_{crit}$ (μg/m$^3$) of gas-phase sulfuric acid that produces a binary $H_2SO_4$-$H_2O$ nucleation rate of 1 p/cm$^3$s (Seinfeld and Pandis 1998):

$C_{crit}$ = 0.16 exp (0.1 T – 3.5 RH – 27.7)

Where RH is the relative humidity (0 to 1) and T is the temperature in K. The empirical equation which fits the $H_2SO_4$-$H_2O$ binary nucleation rate, predicts a critical mass concentration of the order of 0.7-3.5 μg/m$^3$. Assuming nucleation mode particles with mean around 30 nm, this mass concentration corresponds to $10^5$ p/cm$^3$.
Emitted sulfate concentrations can reach 10 mg/m$^3$ at high speeds when an oxidation catalyst is present and high sulfur fuel is used (280 ppm) (Giechaskiel et al. 2007a). If there is no oxidation catalyst sulfate emissions will be lower, e.g., a heavy-duty engine could emit 200 μg/m$^3$ (Shi and Harisson 1999). Thus, the maximum mass concentration at the evaporation tube inlet (after a dilution at the CVS and the primary diluter of the VPR of 5x10) should be less than 200 μg/m$^3$ (with catalyst) or 4 μg/m$^3$ (without catalyst) for vehicles with high sulfur contents. So re-nucleation of sulfuric acid is highly likely.
Assuming a sulfur content of 3–10 ppm for the fuel and 2000–10000 ppm for the lubricant (DieselNet 2013), as well as an oil consumption equivalent to 0.1–0.2% of fuel (DieselNet 2013), one estimates an engine-out $SO_2$ concentration in the range of 0.5-3 ppm. Reported $SO_2$ to $SO_3$ conversion efficiencies for the exhaust temperatures lie in the range of 30–100% for platinum based oxidation catalysts (Giechaskiel et al. 2007a), but much less for palladium based catalysts. Thus the $SO_3$ concentration at the exit of the evaporation tube could be around 0.01-0.3 ppm (assuming a primary dilution of 10) or approximately 10-300 μg/m$^3$. These values are much higher than those required for nucleation.
The nucleation rates can be further enhanced from the release of sulfur previously stored in the oxidation catalyst (Givens et al. 2003; Giechaskiel et al. 2007a), but also due to some ammonia slip. Korhonen et al. (1999) showed that trace amounts of ammonia (5 ppt) may significantly enhance the binary nucleation rate of sulfuric acid and water. The relevance of ammonia in the formation of secondary particles from diesel exhaust was highlighted through both numerical calculations (Lemmetty et al. 2007) but also volatility and hygroscopicity measurements (Meyer & Ristovski 2007). Czerwinski et al. (2009) performed a detailed characterization of the particle emissions of a Euro III heavy-duty diesel engine retrofitted with a DPF followed by an SCR system, and observed the formation of secondary nanoparticles in the SCR that could be detected with a TSI's 3025A PNC downstream of a VPR.
Some studies have shown that re-nucleation can happen in PMP systems with evaporation tube. For example, Mamakos et al. (2013a) and Zheng et al. (2012) found different results <23 nm when they changed the PCRF, due to the different volatile nucleation mode formation and contribution to sub-23 nm concentration. There is no available info regarding the organics or sulfates in their studies but low sulfur fuels were used.

**4) Growth:** The sulfuric acid nucleis are approximately 1-2 nm. They rarely can grow to bigger sizes without existence of hydrocarbons (Du and Yu 2008). With organics they can grow to e.g. 6 nm ($10^{11}$ p/cm organics) (Arnold et al. 2012) or 20 nm ($10^{14}$ p/cm$^3$ hexadecane in 1 s) (Vouitsis et al. 2004). Approximately 1 ppm (or ppv) of propane corresponds to 1.6x$10^{13}$ p/cm$^3$ or 2.4x$10^{13}$ p/cm$^3$. To convert it to typical hydrocarbons found in exhaust gas (e.g. hexadecane) the corresponding molecular weights should be taken into account (e.g. multiply with 44/226). A correction factor 10-30% should also be applied in order to take into account the fraction of total organics potentially condensing on the particulates phase (Vouitsis et al. 2008). The hydrocarbon emissions of modern vehicles with oxidation catalysts are low. However during cold starts at the inlet of the VPR connected to the CVS concentrations of up to 1000 ppm (vehicles) or 30000 ppm (moped) can be measured. Thus the growth of the re-nucleated particles in the 10-20 nm range is very probable.

**5) Quantification of error with lower cut-off:** Typically the re-nucleation mode particles after the evaporation tube will have diameters less than 23 nm, and hence they will not be counted by the PNC. However, if a counter with a lower cut-off size is used, large differences in particle concentrations might be obtained.
In the study of Giechaskiel et al. (2010c) a nucleation mode with concentration $7.0x10^8$ p/cm$^3$, CMD=19.5 nm, σ=1.35 was reduced to $9.0x10^7$ p/cm$^3$, CMD=7 nm, σ=1.35 in a VPR (vehicle with 280 ppm sulfur in the fuel). The accumulation mode of the specific test had concentration $3.0x10^7$ p/cm$^3$, CMD=52 nm, σ=1.95. A PNC with $d_{50\%}$=23 nm would measure 0% of the remaining nucleation mode. A PNC with $d_{50\%}$=10 nm would measure 12% of the remaining nucleation mode which is still a 35% error in the measurement of the non-volatile particles. Thus, lowering the cut-off size of the PNC would be advisable only when low enough concentrations of volatile materials at the inlet of the PN system can be ensured.

Conclusions: The evaporation tube can evaporate volatiles and semi-volatiles. Organics re-nucleation seems unlikely except in the case of mopeds. However the re-nucleation of sulfuric acid is very possible even for low sulfur fuels. The nucleis are in the range of 1-2 nm and can grow to >10 nm depending on the condensation of the available organics. The studies so far have shown that the PMP protocol with the 23 nm cut-point is robust because rarely the particles grow in the >23nm range after the VPR. However reducing the size is not recommended with the existing setup because re-nucleated particles can reach the 10 nm range.

### Thermodenuder

Volatile material can be removed from the exhaust gas by a thermodenuder (Burtscher et al. 2001, Wehner et al. 2002, Huffman et al. 2008). In this case the sample is first heated to a well-defined temperature to evaporate semi-volatile species, and is then passed through an unheated section containing adsorbing material, most often activated carbon, which adsorbs most of the evaporated components and reduces their vapor pressure. The denuder removes the volatile and semi-volatile materials from the gas flow and, therefore, permits much lower dilutions to be used than the evaporation technique. However, dilution is still recommended to decrease concentrations and prolong the lifetime of the active carbon.
The operating temperature of thermodenuders is set around 250°C, which is considered sufficient for nucleation mode elimination (Mayer et al. 1998). Aerosol particles have slower diffusion velocities than the vaporized species, which allows the denuder to preferentially remove gaseous species, but not particles. However, the procedure is more complicated than an evaporation tube and requires more maintenance. The adsorption efficiency of activated carbon decreases with time, and it has to be replaced before breakthrough occurs. However, there is no clear indicator when breakthrough might happen. Particle deposition can also decrease the lifetime of the thermodenuder (Kuo et al. 2013). The thermodenuder incurs particle losses, mainly due to thermophoresis in the adsorbing section, typically about 25-30%. These are mainly size independent, but the additional length of the denuder section increases size-dependent diffusion losses relative to the evaporation tube. Interestingly, special designs with laminar flow can avoid the thermophoretic losses (Fierz et al. 2007). Experimental evidence from the Particulates project gave reasonable results in terms of measurement repeatability utilizing thermodenuders (Ntziachristos et al. 2004a). However, later evidence from the PMP work raised concerns for thermodenuder suitability for solid particles separation in the small particle size range, especially in cases of low solid particle

concentrations or unknown chemical composition (i.e. from DPF equipped vehicles) for regulatory purposes (PMP 2003). Some experimental studies showed that the removal efficiency is not always as high as expected (Giechaskiel et al. 2009a) or even solid particles might be formed (Swanson and Kittelson 2010).

Conclusions: In general, the thermodenuder has the potential for solid particle separation but the active carbon has to be retained far from saturation and dilution should be used to keep the concentration of volatile species low so as to prolong the active carbon lifetime.

### Catalytic stripper (CS)

The catalytic "stripper" (Khalek and Kittelson 1995) has been proposed to be a more effective approach if accurate determination of sub-23 nm solid particles is necessary. The CS utilizes an oxidation catalyst to oxidize volatile hydrocarbons and binds sulfates (chemical approach). These components are removed from the sample flow, thus eliminating the risk for subsequent nucleation or recondensation.
The first CS (Khalek and Kittelson 1995) consisted of a commercial oxidation catalyst heated to 300°C that was followed by a cooling coil tube to reduce temperature to ambient levels. The CS was shown to efficiently remove hydrocarbons and ammonium sulfate. Subsequent work combined a similar CS with a downstream vortex tube diluter to minimize thermophoretic losses (Khalek 2007). Recently a downsized CS replaced the evaporation tube in a PMP compliant system, and was found to meet the legislation requirements and removed up to 70 nm tetracontane particles with efficiency of >99% (Khalek and Bougher 2011), while the removal efficiency of a PMP system of such big particles was 90%.
Another version of the CS employed a sulfur trap upstream of the catalyst to protect the oxidation catalyst from $SO_2$ adsorption (Stenitzer 2003). The system was used to investigate the non-volatile part of vehicle emissions (Kittelson et al. 2005, Zheng et al. 2011) and was recently found superior to a thermodenuder (Swanson and Kittelson 2010). Recently a new 'advanced' CS was introduced which consists of an oxidation catalyst followed by a sulfur trap (Giechaskiel et al. 2010a, Swanson et al. 2013), and was found superior to the PMP method for sub-23 nm particles (Amanatidis et al. 2013, Ntziachristos et al. 2013).
In one study (Amanatidis et al. 2013) the CS was capable of fully oxidizing hydrocarbon species even at particularly high concentrations, achieving a conversion of more than 99% in all cases. The maximum hydrocarbons concentration used (>4% v/v) was much beyond any level that the CS could be exposed at in combustion aerosol measurements. For example, 2-stroke mopeds are amongst the highest combustion sources of hydrocarbons with levels reaching 50 $mg/m^3$ in the CVS or 700 $mg/m^3$ in the raw exhaust (Giechaskiel et al. 2010c). The CS was challenged with 4% v/v hydrocarbon concentration or 26000 $mg/m^3$ which was more than 35 times higher than the raw exhaust moped emission level.
The removal efficiency of a CS was 96% for 30 nm tetracontane particles and further decreased at larger sizes, for CS operation at 300°C and a flowrate of 1.5 lpm (Amanatidis et al. 2013). This shows that the specific CS alone was not compliant with the legislation (PMP) requirements (>99% removal of >30 nm tetracontane particles). The removal efficiency was increased to >99% when the temperature of the CS was raised to 350°C, or when heating the sample at 250°C prior to the CS or when the residence time in the CS was increased (0.3 lpm flowrate). The removal efficiency with pre-heating and high residence time (0.3 lpm) was found 99.6% even when the CS was challenged with a high concentration of large particles ($1.3x10^5$ $p/cm^3$ at 75 nm). In another study (Swanson et al. 2013), the CS fully removed monodisperse tetracontane particles as large as 220 nm at a concentration of 10000 $p/cm^3$.

Tetracosane particles can be removed even more easily (Swanson and Kittelson 2010). These results, combined with the gas hydrocarbon breakthrough tests, indicate that the removal of hydrocarbons in the gaseous phase is much more efficient than their removal in the particulate phase. This is consistent with the much higher mass transfer rates of gases than particles to the catalyst surface.
Evaluation of the CS with sulfuric acid also showed high removal rates. Sulfuric acid re-nucleation was not observed until the challenge concentration was higher than 10 mg/m$^3$ (Swanson et al. 2013). In another study the sulfur storage capacity was estimated to be approximately 6.1 mg or 0.68 g/liter of catalyst volume (Amanatidis et al. 2013). However, particle size distribution measurements downstream of the CS revealed that sulfate particle formation was initialized after exposure to sulfur ($SO_2$). Particle size gradually grew with time, starting from 5 nm geometric mean diameter to reach 50 nm, following the increase and stabilization in outlet $SO_2$ concentration. Hence, the sulfur storage capacity before sulfate particle formation could be detected was approximately 2.4 mg, i.e. only about 40% of total sulfur storage capacity. The minimum sulfur capacity identified in that study (2.4 mg) corresponded to an exposure of the CS in raw exhaust for approximately 3000 km of driving distance. Considering that the European type-approval driving cycle (NEDC) is around 11 km and lasts for 20 min, the CS would be saturated in approximately 90 h of operation in raw exhaust. This value increases proportionally with dilution upstream of the CS. For example, the dilution ratio upstream of the CS would be at least 100:1 in typical PMP application (i.e. sampling downstream of a CVS and a primary diluter), thus increasing the CS operation time to 9000 h or 300.000 km of driving distance before any sulfate particles would be detected. Typically the losses of CS are due to diffusion and thermophoressis. Without any dilution downstream of the CS, they are around 25% for 50-100 nm particles. With dilution they are 5-10%. The 50% penetration is around 10 nm (Amanatidis et al. 2013, Swanson et al. 2013).

Conclusions: In general, the CS appears to handle higher semi-volatile concentrations more effectively than the thermodenuder and evaporation tube. On the other hand, particle losses are somewhat larger than the other methods. The risk to form sulfate particles due to the oxidative environment in the CS may pose a limitation in exhaust aerosol treatment, especially when high sulfur fuels (i.e. >100 ppm) are used, such as is still in use in several Asian counties. Introduction of such a system in the legislation needs extra specifications. For example, the procedures for the evaluation of the oxidation efficiency have to be determined (e.g. a specific hydrocarbon at a specific concentration). The onsite periodic check of the oxidation efficiency is also desirable. Another important characteristic is the $SO_2$ to $SO_3$ conversion. A high conversion ratio might create nucleation mode particles due to sulfuric acid nucleation that under a normal PMP system wouldn't appear (the $SO_2$ doesn't nucleate). A very critical requirement is the sulfur storage capacity. This could be checked with $SO_2$ gas analyzer or with particle measurements. However, when the CS is sulfur saturated it cannot be used, unless regenerated. Thus, there is no simple way to check this onsite. The sulfur storage life time depends on engine conditions and dilution ratios used and thus is extremely difficult even to estimate it during the real life operation of the system.

## Experimental investigation at JRC (Artifacts <23 nm)

In order to investigate the robustness of the PMP protocol some tests were conducted with a DPF vehicle during regeneration and a moped.

## Regeneration

During regeneration high temperatures are encountered and volatile material desorbs from the tailpipe and the aftertreatment devices. Figure 9 shows the emissions during such an event:

- Particles >23 nm after a VPR with evaporation tube (ET) (PMP protocol) (connected to the CVS).
- Particles >23 nm after a VPR with evaporation tube (ET) (PMP protocol) but connected to the tailpipe.
- Particles >3 nm after a VPR with evaporation tube (ET) (connected to the CVS),
- Particles >6 nm after a VPR with evaporation tube (ET) but connected to the tailpipe (with an EEPS).

The PMP emissions at the CVS and the tailpipe are identical. The same applies for the >6 nm emissions. However the >3 nm emissions are extremely high indicating that particles were formed inside the VPR. These volatiles that re-nucleated in the VPR originate mainly from the vehicle because other systems connected at the tailpipe without thermal pretreatment also had such high increase of concentration (not shown). Since the EEPS that measures >6 nm couldn't detect them, it means that the nucleation mode remained at low sizes (<6 nm).

## Moped

Traditional two-stroke engines are not highly efficient because the scavenging phase loses up to 30% of the unburned fuel/oil mixture into the exhaust. In addition, a portion of the exhaust gas remains in the combustion chamber during the cycle. These inefficiencies contribute to power loss when compared with 4-stroke engines but also to a high amount of unburned fuel. Thus, in the case of mopeds, the VPR is exposed to very high concentrations of semi-volatile material.
Figure 10 shows the particle emissions over the 8 (identical) phases of the ECE-47 cycle for different protocols:

- Total particles >3 nm
- Particles >3 nm after a VPR with evaporation tube (ET),
- Particles >3 nm after a VPR with evaporation tube (ET) and a catalytic stripper (CS),
- Particles >23 nm after a VPR with evaporation tube (ET) (PMP protocol).

As it can be seen, after the VPR the >3 nm particle emissions are much higher compared to those in the CVS tunnel (Total). This indicates formation of particles in the VPR (after the ET). Note that the dilution was >15 at the CVS even at the maximum speed of the moped, the primary dilution of the PMP system was 1000 and the secondary 10. Thus the artifact could be observed even with very high dilution. These particles could be removed with a catalytic stripper (CS). Note that the PMP protocol (which measures > 23 nm) gives the correct result and can be considered robust.

Conclusions: The PMP protocol is robust but lowering the cut-off size might lead to wrong results (i.e. measuring volatiles as solid particles) at specific cases like regeneration of DPFs and mopeds. The limited tests conducted here indicate that the re-nucleated particles are usually small in size, but can happen during regeneration or mopeds, in agreement with the theoretical estimations at the previous section.

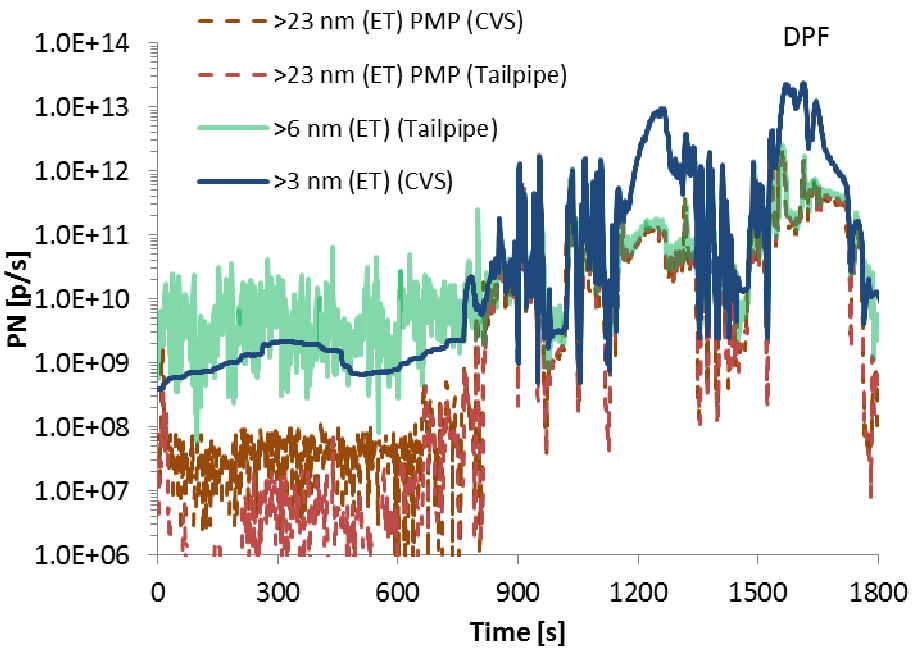


**Figure 9:** *Emissions during a regenerating WLTP cycle.*

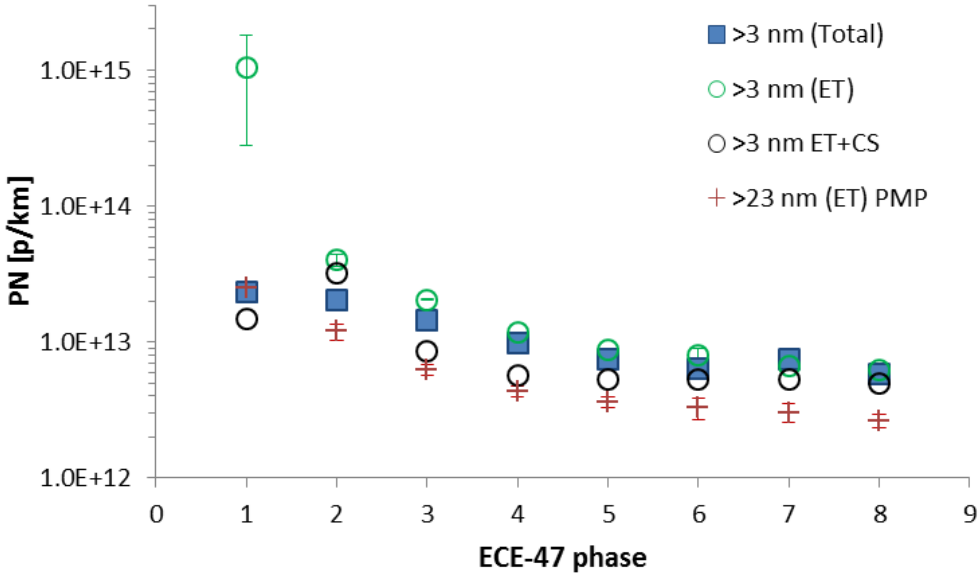


**Figure 10:** *Emissions of a moped.*

## Summary and conclusions

Particle Number (PN) systems consist of a Volatile Particle Remover (VPR) and a Particle Number Counter (PNC). The VPR removes volatile particles and dilutes the sample. The PNC measures the number concentration of particles >23 nm to exclude possible confounding of measurements by low volatility hydrocarbons present as nucleation mode particles, while including the primary soot (spherule) size of 23 nm.
Target of this report was to investigate whether it is necessary and possible to measure <23 nm particles. In other words it was investigated 1) whether smaller <23 nm solid particles are emitted by engines in considerable concentration focusing on Gasoline Direct Injection (G-DI) engines, 2) whether all volatile particles can be removed efficiently with the existing method, 3) whether any artifacts can happen (e.g. formation of non-volatile particles due to pyrolysis) and 4) whether a lower than 23 nm size increases significantly the measurement uncertainty.

**Health effects**
Although the total mass still correlates best with adverse health effects, surface area might be more important. Each part of the total mass (soluble and insoluble fraction) has its contribution. Metal oxides also contribute significantly. The size of particles determines the deposition location and deposition fraction. It increases with decreasing size. Thus legislating <23 nm solid particles is important if vehicles emit high concentration not detected with the current method and/or the nature of this particles is proven to be dangerous for human health.

**Primary particles and size distributions**
The mean value of the primary particles is around 25 nm. No significant differences were observed for G-DI particles. However the following points should be considered for G-DIs: The distribution of particles and primary particles can be wider, so larger percentage of particles <23 nm can exist. The structure of primary particles is sometimes different (more amorphous) probably due to unburned hydrocarbons or volatile organics due to fuel impingement at early fuel injection time. This means that differences in the thermal pre-treatment (temperature, residence time of PN systems) might lead to different results.

**Solid <23 nm particles (review)**
A solid nucleation mode has been measured with older and modern diesel engines. It appears mostly at low loads but even at high. Solid nucleation mode is often observed at gasoline engines with port fuel injection (G-PFI) and it is assumed to originate from the metals of the lube oil or from fuel additives. Thus cases with fuel or lubricant (metal) additives or high lubricant consumption need special attention. At G-DIs a shoulder at 20 nm appears quite often. A separate solid nucleation mode is not typical, but the size distribution can peak at small sizes (20 nm or lower) in some engine operation modes (although very unusual). For mopeds very often the size distribution after thermal pre-treatment peaks at or below 20 nm. It should be mentioned that in many studies it was recognized that the 'solid' nucleation mode was artifact of the PMP method and the dilution factors employed.

**Experimental investigation at JRC (Solids <23 nm)**
Tests at JRC showed that for emission levels around $10^{12}$ p/km, the percentage of particles not measured (i.e. <23 nm) is <20% for Diesel with DPF vehicles and <60% for G-DIs. Extending

the PMP to 10 nm will capture one part of the solid nucleation mode which peaks around 10 nm. Extending the PMP protocol as it is to 5 nm particles can result in wrong measurements due to re-nucleation.

**Feasibility of sub 23 nm measurement for PNCs**

Lowering the cut-off size of the PNC is feasible and probably advantageous (less dependence on particles' material) for the calibration and the actual emission measurements. The cut-off size of existing PNCs can change (permanently or interchangeably) down to 10 nm relatively easily. Lower than 10 nm cut-off sizes need different designs of PNCs that do not necessarily fit in the existing VPRs. For lower than 10 nm cut-off sizes, the calibration material has to be re-investigated, because it's not so easy to produce small (emery oil) particles at high enough concentrations.

**Feasibility of sub 23 nm measurement for VPRs**

*Penetration:* The losses in the VPRs increase significantly with decreasing size. Measurement is possible down to approximately 10 nm only as indication of existence of particles (the accurate quantification is extremely difficult). Even in that case the PCRF determination should remain based on monodisperse particles of 30, 50 and 100 nm. The material for the approximately 10 nm VPR calibration point has to be investigated.

*Impact on measurement error:* Lowering the cut-off size of the systems can increase the measurement uncertainty for two reasons: 1) The used mean PCRF might be a non-representative average for the measured size distributions. 2) The differences between commercial systems will increase due to different penetrations at lower sizes. The first issue can be minimized by continuing using the mean of 30, 50 and 100 nm particles and the second by giving permitted ranges of penetrations for smaller particles. Theoretical calculations showed that byy lowering the cut-off size, the measurement uncertainty due to differences in the penetrations of commercial systems will not be affected for typical size distributions (between 50 and 90 nm). However, for smaller than 50 nm means, the uncertainty is expected to increase, due to the differences of the penetration curves of the commercial systems.

*Formation of solids:* There are indications that solid particles can be formed by hydrocarbons and sulfuric acid in the evaporation tube but this needs further investigation.

*Volatile Removal efficiency:* The evaporation tube can evaporate volatiles and semi-volatiles. Organics re-nucleation seems unlikely except in the case of mopeds. However the re-nucleation of sulfuric acid is very possible even for low sulfur fuels. The nucleis are in the range of 1-2 nm and can grow to >10 nm depending on the condensation of the available organics. The studies so far have shown that the PMP protocol with the 23 nm cut-point is robust because rarely the particles grow in that range after the VPR. However reducing the size is not recommended with the existing setup.

The CS appears to handle higher semi-volatile concentrations more effectively than the thermodenuder and evaporation tube. On the other hand, particle losses are somewhat larger than the other methods. The risk to form sulfate particles due to the oxidative environment in the CS may pose a limitation in exhaust aerosol treatment, especially when high sulfur fuels (i.e. >100 ppm) are used, such as is still in use in several Asian counties. Introduction of such a system in the legislation needs extra specifications and requirements.

**Experimental investigation at JRC (Artifacts <23 nm)**
The PMP protocol is robust but lowering the cut-off size might lead to wrong results (i.e. measuring volatiles as solid particles) at specific cases like re-generation and mopeds. The limited tests conducted at JRC indicate that the re-nucleated particles are usually small in size, but can happen during regeneration or mopeds.

**Main conclusion**
Based on the results of this review at the moment there is not enough data to support a change of the legislation: The PMP procedure should remain as it is. However due to increased <23 nm solid particle emissions in some cases (additives in fuel or lubricant, special calibration of an engine etc.) sub-23 nm particles should be monitored.

**Proposal for tests and experimental conditions**
When sub-23 nm measurements are conducted a CS should be used. Without CS the measurements should be conducted with as high as possible primary dilution (PCRF). In case of extreme differences between >23 nm and <23 nm particles, the measurement should be repeated with 10 times higher primary dilution (PCRF). Due to extreme losses in the sub-10 nm range and the possibility of artifacts (re-nucleation or pyrolysis) for legislation reasons the sub-10 nm are not recommended. Whenever possible, the nature of the sub-23 nm particles should be investigated (see Annex D).

# References


Alföldy B., Giechaskiel B., Hofmann W., & Drossinos, Y. (2009). Size-distribution dependent lung deposition of diesel exhaust particles. J. Aerosol Sci. 40, 652-663

Alger T., Gingrich J., Khalek I., & Mangold B. (2010). The role of EGR in PM emissions from gasoline engines. SAE 2010-01-0353

Amanatidis, S., Ntziachristos, L., Giechaskiel, B., Katsaounis, D., Samaras, Z., & Bergmann, A. (2013). Evaluation of an oxidation catalyst ("catalytic stripper") in eliminating volatile material from combustion aerosol. J. Aerosol Sci., 57, 144-155.

Andersson J., Giechaskiel B., Munoz-Bueno R., & Dilara P. (2007). Particle measurement programme (PMP): Light-duty inter-laboratory correlation exercise (ILCE_LD)-Final report (EUR 22775 EN) GRPE-54-08-Rev.1, http://publications.jrc.ec.europa.eu/repository/bitstream/111111111/429/2/7386%20-%20PMP_LD_final.pdf

Andersson J., Wedekind B., Hall D., Stadling R., & Wilson G. (2001). DETR/SMMT/CONCAWE particulate research programme: Light duty results, SAE 2001-01-3577.

Armas O., Garcia-Contreras R., Ramos A. (2013). Emissions of light duty vehicle tested under urban and extraurban real-world driving conditions with diesel, animal fat biodiesel and GTL fuels. SAE 2013-24-0176

Armas O., Gómez A., Mata C., & Ramos Á. (2012). Particles emitted during the stops of an urban bus fuelled with ethanol-biodiesel-diesel blends. Urban Climate, 2, 43-54

Arnold F., Pirjola L., Rönkkö T., Reichl U., Schlager H., Lähde T., Heikkilä J., & Keskinen J. (2012). First online measurements of sulphuric acid gas in modern heavy-duty diesel engine exhaust: implications for nanoparticle formation. Eniron. Sci. TEchnol. 46, 11227-11234

Barone T.L., Storey J.M.E., Youngquist A.D., & Szybist J.P. (2012). An analysis of direct-injection spark-ignition (DISI) soot morphology. Atmospheric Environment, 49, 268-274.

Bérubé K.A., Jones T.P., Williamson B.J., Winters C., Morgan A. J., & Richards R. J. (1999). Physicochemical characterisation of diesel exhaust particles: Factors for assessing biological activity. Atmospheric Environment, 33, 1599-1614.

Biswas S., Hu S., Verma V., Herner J., Robertson W., Ayala A., & Sioutas C., (2008). Physical properties of particulate matter (PM) from late model heavy-duty diesel vehicles operating with advanced PM and $NO_x$ emission control technologies. Atmospheric Environment, 42, 5622-5634.

Bosteels D., May J., Karlsson H., & de Serves C. (2006). Regulated and non-regulated emissions from modern European passenger cars, SAE 2006-01-1516.

Braisher M., Stone R., & Price P. (2010). Particle number emissions from a range of European vehicles, SAE 2010-01-0786.

Brown D.M., Wilson M.R., MacNee W., Stone V., & Donaldson K. (2001). Size-dependent pro-inflammatory effects of ultrafine polystyrene particles: A role for surface area and oxidative stress in the enhanced activity of ultrafines. Toxicology and Applied Pharmacology, 175, 191-199.

Burtscher H., Baltensperger U., Bukowiecki N., Cohn P., Hüglin C., Mohr M., Matter U., Nyeki S., Schmatloch V., Streit N., & Weingartner E. (2001). Separation of volatile and non-volatile aerosol fractions by thermodesorption: instrumental development and applications. J. Aerosol Sci., 32, 427-442.

Burtscher H., Matter U., Skillas G., & Zhiqiang Q. (1998). Particles in diesel exhaust caused by fuel additives. J. Aerosol Sci. 29, Suppl. 1, 955-956

Burwell R.L., Scott R.B., Maury L.G., & Hussey A.S. (1954). The action of 96% sulphuric acid on alkanes at 601. J. American Chemical Society, 76, 5822–5827.

Bzdek B., Pennington R., & Johnston M. (2012). Single particle chemical analysis of ambient ultrafine aerosol: a review. J. Aerosol Sci., 52, 109-120.

Cauda E., Fino D., Saracco G., & Specchia V. (2007). Secondary nanoparticle emissions during diesel particulate trap regeneration. Topics in Catalysis, 42-43, 253-257

Cauda E., Hernadez S., Fino D., Saracco G., & Specchia V. (2006). PM0.1 emissions during diesel trap regeneration. Env. Sci. Techn., 40, 5532-5537

Cheung K., Andrea P., Ntziachristos L., Samaras Z., Cassee F., Gerlofs M., & Sioutas, C. (2009). Chemical characteristics and oxidative potential of particulate matter emissions from gasoline, diesel, and biodiesel cars. Environ. Sci. Technol. 43, 6334-6340

Cho A., Sioutas C., Miguel A., Kumagai Y., Schmitz D., Singh M., Eiguren-Fernandez A., & Froines J. (2005). Redox activity of airborne particulate matter at different sites in the Los Angeles Basin. Environ. Res. 99, 40–47

Cross E., Sappok A., Fortner E., Hunter J., Jayne J., Wong V., Trimborn A., Worsnop D., Kroll J., Brooks W., & Onasch T. (2012). Real-time measurements of engine-out trace elements: application of a novel soot particle aerosol mass spectrometer for emissions characterization. J. Eng. Gas Turbines Power 134 (7), 072801

Czerwinski J., Comte P., Larsen B., Martini G., Mayer A. (2006). Research on particle emissions of modern 2-stroke scooters. SAE 2006-01-1078.

Czerwinski J., Comte P., Reutimann F. (2005). Nanoparticle emissions of a DI 2-stroke scooter with varying oil- & fuel quality. SAE 2005-01-1101.

Czerwinski J., Zimmerli Y., Mayer A., Heeb N., Lemaire J., D'Urbano G., & Bunge R. (2009). Testing of combined DPF and SCR Systems for HD-retrofitting—VERTdePN. SAE Technical Paper 2009-01-0284.

Czerwinski, J., Comte, P., Mayer, A., and Reutimann, F. (2013). Investigations of changes of the 2-stroke scooters nanoparticles in the exhaust- and CVS-system. SAE 2013-24-0178

De Filippo A., & Maricq M. (2008). Diesel nucleation mode particles: Semivolatile or solid? Environ Sci. Technol., 42, 7957-7962

Dick C., Brown D., Donaldson K. & Stone V. (2003). The role of free radicals in the toxicity and inflammatory effects of four ultrafine particle types. Inhalation Toxicology 15, 39-52

Diesel Net (2013). http://www.dieselnet.com/

Donaldson K., & MacNee W. (2001). Potential mechanisms of adverse pulmonary and cardiovascular effects of particulate air pollution. International Journal of Hygiene and Environmental Health, 203, 411-415.

Donaldson K., Li X., & MacNee W. (1998). Ultrafine (nanometre) particle mediated lung injury. J. Aerosol Sci. 29, 553–560

Du H., & Yu F. (2008). Nanoparticle formation in the exhaust of vehicles running on ultra-low sulphur fuel. Atmos. Chem. Phys. 8, 4729-4739

Dwyer H., Ayala A., Zhang S., Collins J., Huai T., Herner J., & Chau W. (2010). Emissions from a diesel car during regeneration of an active diesel particulate filter. J. Aerosol Sci., 41, 541-552

Dwyer H., Ayala A., Zhang S., Collins J., Huai T., Herner J., & Chau W. (2010). A study of emissions from a Euro 4 light duty diesel vehicle with the European particulate measurement programme. Atmospheric Environment, 44, 3469-3476

EPA (2009). Integrated science assessment for particulate matter (final report). U.S. Environmental Protection Agency, Washington, DC, EPA/600/R-08/139F, 2009. http://cfpub.epa.gov/ncea/cfm/recordisplay.cfm?deid=216546#Download

Etissa D., Mohr M., Schreiber D., Buffat P.A. (2008). Investigation of particles emitted from modern 2-stroke scooters. Atmospheric Environment 42, 183–95.

Ferin J., Oberdörster G., & Penney D. (1992). Pulmonary retention of ultrafine and fine particles in rats. American Journal of Respiratory Cell and Molecular Biology 6, 535–542

Fierz M., Vernooij M., & Burtscher H. (2007). An improved low-flow thermodenuder. J. Aerosol Sci., 38, 1163-1168.

Fushimi A., Saitoh K., Fujitani Y., Hasegawa S., Takahashi K., Tanabe K., & Kobayashi S. (2011). Organic-rich nanoparticles (diameter 10-30 nm) in diesel exhaust: Fuel and oil contribution on chemical composition. Atmospheric Environment 45, 6326-6336

Gaddam G., & Vander Wal R. (2013). Physical and chemical characterization of SIDI engine particulates. Combustion and Flame 160, 2517-2528

Gard E., Mayer J., Morrical B., Dienes T., Fergenson D., & Prather K. (1997). Real-time analysis of individual atmospheric aerosol particles: design and performance of portable ATOFMS. Anal. Chem., 69, 4083- 4091.

Gauderman W., Avol E., Gilliland F., Vora H., Thomas D., Berhane K., McConnell R., Kuenzli N., Lurmann F., Rappaport E., Margolis H., Bates D., & Peters J. (2004). The effect of air pollution on lung development from 10 to 18 years of age. New England Journal of Medicine 351(11), 1057-1067

Geller M., Ntziachristos L., Mamakos A., Samaras Z., Schmitz D., Froines J., & Sioutas, C. (2006). Physicochemical and redox characteristics of particulate matter (pm) emitted from gasoline and diesel passenger cars. Atmospheric Environment 40, 6988–7004

Gidney J., Twigg M., & Kittelson D. (2010). Effect of organometalic fuel additives on nanoparticle emissions from a gasoline passenger car. Environ. Sci. Technol., 44, 2562-2569.

Giechaskiel B., & Drossinos Y. (2010). Theoretical investigation of volatile removal efficiency of particle number measurement systems. SAE 2010-01-1304.

Giechaskiel B., Alföldy B., & Drossinos, Y. (2009d). A metric for health effect studies of diesel aerosol particles. J. Aerosol Sci. 40, 639-651

Giechaskiel B., Bergmann A., Liu Z., Zheng Z., Jung H., Johnson K., Swanson J., Kittelson D., Hu S., & Huai T. (2010a). Evaluation of the European method and the catalytic stripper for particle number measurements. AAAR 29th Conference, Portland, USA, October 25-29, 2010.

Giechaskiel B., Carriero M., Martini G., & Andersson J. (2009c). Heavy duty particle measurement programme (PMP): exploratory work for the definition of the test protocol. SAE 2009-01-1767.

Giechaskiel B., Carriero M., Martini G., Bergmann A., Pongratz H., & Jörgl H. (2010b). Comparison of particle number measurements from the full dilution tunnel, the tailpipe and partial flow systems, SAE 2010-01-1299.

Giechaskiel B., Carriero M., Martini G., Krasenbrink A., & Scheder D. (2009a). Calibration and validation of various commercial particle number measurement systems. SAE 2009-01-1115

Giechaskiel B., Chirico R., DeCarlo P., Clairotte M., Adam T., Martini G., Heringa M., Richter R., Prevot A., Baltensperger U., & Astorga C. (2010c). Evaluation of the particle measurement programme (PMP) protocol to remove the vehicles' exhaust aerosol volatile phase. Sci. Total Environment, 408, 5106-5116.

Giechaskiel B., Cresnoverh M., Jörgl H., & Bergmann A. (2010d). Calibration and accuracy of a particle number measurement system. Meas. Sci. Technol. 21:045102.

Giechaskiel B., Dilara P., & Andersson J., (2008a). Particle measurement programme (PMP) light-duty inter-laboratory exercise: Repeatability and reproducibility of the particle number method, Aerosol Sci. Technol. 42:528-543.

Giechaskiel B., Mamakos A., Andersson J., Dilara P., Martini G., Schindler W., & Bergmann A. (2012). Measurement of automotive non-volatile particle number emissions within the European legislative framework: a review. Aerosol Sci. Technol., 46, 719-749.

Giechaskiel B., Maricq M., Ntziachristos L., Dardiotis C., Wang X., Axmann H., Bergmann A., Schindler W. (2014). Review of motor vehicle particulate emissions sampling and measurement: From smoke and filter mass to particle number. J. Aerosol Sci. 67, 48–86.

Giechaskiel B., Martinez-Lozano P., Alessandrini S., Forni F., Montigny F., Fumagalli I., Carriero M., & Martini G., (2008b). Particle measurement programme (PMP) heavy duty (HD) inter-laboratory exercise: Validation exercise tests at JRC (Feb 08). EU report 23496.

Giechaskiel B., Ntziachristos L., Samaras Z., Casati R., Scheer V., & Vogt R. (2005). Formation potential of vehicle exhaust nucleation mode particles on-road and in the laboratory. Atmospheric Environment, 39, 3191-3198.

Giechaskiel B., Ntziachristos L., Samaras Z., Casati R., Scheer V., & Vogt R. (2007a). Effect of speed and speed transition on the formation of nucleation mode particles from a light duty diesel vehicle. SAE 2007-01-1110.

Giechaskiel B., Wang X., Gilliland D., & Drossinos Y. (2011). The effect of particle checmical composition on the activation probability in n-butanol condensation particle counters. J. Aerosol Sci. 42, 20–37

Giechaskiel B., Wang X., Horn H., Spielvogel J., Gerhart C., Southgate J., Jing L., Kasper M., Drossinos Y., & Krasenbrink A. (2009b). Calibration of condensation particle counters for legislated vehicle number emission measurements. Aerosol Sci. Technol., 43, 1164-1173.

Givens W.A., Buck W.H., Jackson A., Kaldor A., Hertzberg A., Moehrmann W., Mueller-Lunz S., Pelz N., & Wenninger G,. (2003). Lube formulation effects on transfer of elements to exhust after-treatment system components. SAE 2003-01-3109.

Gojova A., Guo B., Kota R., Rutledge J., Kennedy I., & Barakat A. (2007). Induction of inflammation in vascular endothelial cells by metal oxide nanoparticles: effect of particle composition. Environmental Health Perspectives 115, 3, 403-409

Gupta T., Kothari A., Srivastava D., & Agarwal A. (2010). Measurement of number and size distribution of particles emitted from a mid-sized transportation multipoint port fuel injection gasoline engine. Fuel, 89, 2230-2233

Hall D., & Dickens C. (1999). Measurement of the number and size distribution of particles emitted from a gasoline direct injection vehicle, SAE 1999-01-3530.

Harris S., & Maricq M. (2001). Signature size distributions for diesel and gasoline engine exhaust particle matter, J. Aerosol Sci. 32:749–764.

He X., Ratcliff M., & Zigler B. (2012). Effects of gasoline direct injection engine operating parameters on particle number emissions. Energy & Fuels, 26, 2014-2027

Hedge M., Weber P., Gingrich J., Alger T., & Khalek I. (2011). Effect of EGR on particle emissions from a GDI engine. SAE 2011-01-0636

Heikkilä J., Rönkkö T., Lähde T., Lemmetty M., Arffman A., Virtanen A, Keskinen J., Pirjola L., & Rothe D. (2009). Effect of open channel filter on particle emissions of modern diesel engine, Journal of the Air & Waste Management Association, 59:10, 1148-1154

Hermann M., Wehner B., Bischof O., Han H.-S., Krinke T., Liu W., Zerrath A., & Wiedensohler A. (2007). Particle counting efficiencies of new TSI condensation particle counters. J. Aerosol Sci., 38, 674-682

Herner J., Hu S., Robertson W., Huai T., Chang O., Rieger P., & Ayala A. (2011). Effect of advanced aftertreatment for PM and $NO_x$ reduction on heavy-duty diesel engine ultrafine particle emissions. Environ. Sci. Technol., 45, 2413-2419.

Herner J., Robertson W., & Ayala A. (2007). Investigation of ultrafine particle number measurements from a clean diesel truck using the European PMP protocol. SAE 2007-01-1114

Huang C., Lou D., Hu Z., Feng Q., Chen Y., Chen C., Tan P. & Yao D. (2013). A PEMS study of the emissions of gaseous pollutants and ultrafine particles from gasoline- and diesel-fueled vehicle. Atmospheric Environment, 77, 703-710

Huang C., Lou D., Hu Z., Tan P., Yao D., Hu W., Li P., Ren J., & Chen C. (2012). Ultrafine particle emission characteristics of diesel engine by on-board and test bench measurement. J. Environmental Sciences 24, 1972-1978

Huffman A., Ziemann P., Jayne J., Worsnop D., & Jimenez J. (2008). Development and characterization of a fast-stepping/scanning thermodenuder for chemically-resolved aerosol volatility measurements. Aerosol Sci. Technol., 42, 395-407.

ICRP 1994. Human respiratory tract model for radiological protection. International Commission on Radiological Protection (ICRP) Publication 66, Pergamon Press, Oxford.

Jayne J., Leard D., Zhang X., Davidovits P., Smith K., Kolb C., and Worsnop D. (2000). Development of an aerosol mass spectrometer for size and composition analysis of submicron particles. Aerosol Sci. Technol., 33, 49-70.

Jeng H., & Swanson J. (2006). Toxicity of metal oxide nanoparticles in mammalian cells. J Environ Sci Health A Tox Hazard Subst Environ Eng. 41 (12), 2699-711.

Johansson A., Hemdal S., & Dahlander P. (2013). Experimental investigation of soot in a spray-guided single cylinder GDI engine operating in a stratified mode. SAE 2013-24-0052

Johnson K. C., Durbin T. D., Jung H., Chaudhary A., Cocker D. R., Herner J. D., Robertson W. H., Huai T., Ayala A., & Kittelson D. (2009). Evaluation of the European PMP methodologies during on-road and chassis dynamometer testing for DPF equipped heavy-duty diesel vehicles. Aerosol Sci. Technol. 43, 962-969.

Johnston M. (2000). Sampling and analysis of individual particles by aerosol mass spectrometry. J. Mass Spectrom., 35, 585-595.

Jung H., Guo B., Anastasio C., & Kennedy I.M. (2006). Quantitative measurements of the generation of hydroxyl radicals in a surrogate lung fluid. Atmospheric Environment, 40, 1043-1052.

Jung H., Kittelson D., &Zachariah M. (2005). The influence of a cerium additive on ultrafine diesel particle emissions and kinetics of oxidation. Combustion and flame. 142, 276-288

Karlsson H. (2005). Measurement of emissions from four diesel fuelled passenger cars meeting Euro 4 emission standards. Report No MTC 5505, AVL MTC AB, 2005/10, Haninge, Sweden.

Karlsson H., Gustafsson J., Cronholm P., & Möller L. (2009). Size-dependent toxicity of metal oxide particles - A comparison between nano- and micrometer size. Toxicology Letters 188, 112–118

Kesten J., Reineking A., & Porstendörfer J. (1991).Calibration of a TSI model 3025 ultrafine condensation particle counter, Aerosol Sci. Technology, 15, 107-111

Khalek I. (2007). Sampling system for solid and volatile exhaust particle size, number, and mass emissions. SAE 2007-01-0307.

Khalek I., & Bougher T. (2011). Development of a solid exhaust particle number measurement system using a catalytic stripper technology. SAE 2011-01-0635.

Khalek I., & Kittelson D. (1995). Real time measurement of volatile and solid exhaust particles using a catalytic stripper. SAE 950236.

Khalek I., Bougher T., & Jetter J., (2010). Particle emissions from a 2009 gasoline direct injection engine using different commercially available fuels, SAE 2010-01-2117.

Khalek I., Kittelson D., & Brear F. (1999). The influence of dilution conditions on diesel exhaust particle size distribution measurements. SAE 1999-01-1142.

Khalek I., Kittelson D., & Brear F. (2000). Nanoparticle growth during dilution and cooling of diesel exhaust: experimental investigation and theoretical assessment. SAE 2000-01-0515.

Khalek I., Kittelson D., Graskow B., Wei Q., & Brear F. (1998). Diesel exhaust particle size: measurements, issues and trends. SAE 980525.

Kim H., & Choi B. (2008). Effect of ethanol-diesle blend fuels on emission and particle size distribution in a common-rail direct injection diesel engine with warm-up catalytic converter. Renewable Energy 33, 2222-2228

Kittelson D. B. Engines and nanoparticles: A review.(1998). J. Aerosol Sci., 29, 575-588.

Kittelson D., Dolan D., Diver R., & Aufderheide E. (1978). Diesel exhaust particle size distributions - fuel and additive effects. SAE 780111.

Kittelson D., Watts W., & Johnson J. (2006a). On-road and laboratory evaluation of combustion aerosols. Part1: summary of diesel engine results. J. Aerosol Sci., 37, 913-930.

Kittelson D., Watts W., & Johnson J. (2006b). On-road and laboratory evaluation of combustion aerosols. Part2: summary of spark ignition engine results. J. Aerosol Sci., 37, 931-949.

Kittelson D., Watts W., Johnson J., Thorne C., Higham C., Payne M., Goodier S., Warrens C., Preston H., Zink U., Pickles D., Goersmann C., Twigg M., Walker A., & Boddy R. (2008). Effect of fuel and lube oil sulfur on the performance of a diesel exhaust gas continuously regenerating trap. Environ. Sci. Technol., 42, 9276-9282.

Kittelson D., Watts W., Savstrom J., & Johnson J. (2005). Influence of a catalytic stripper on the response of real time aerosol instruments to diesel exhaust aerosol. J. Aerosol Sci., 36, 1089-1107.

Kochbach A., Johansen B., Schwarze P., & Namork E. (2005). Analytical electron microscopy of combustion particles: a comparison of vehicle exhaust and residential wood smoke. Sci. Total Environ. 346, 231-243

Korhonen P., Kulmala M., Laaksonen A., Viisanen Y., McGraw R., & Seinfeld J.H (1999). Ternary nucleation of H2SO4, NH3, andH2O in the atmosphere. Journal of Geophysical Research, 104, 26349–26354.

Kuo Y., Lin C., Huang S., Chang K., & Chen C. (2013). Effect of aerosol loading on breakthrough characteristics of activated charcoal cartridges. J. Aerosol Sci., 55, 57-65.

Kwon S. B., Lee K. W., Saito, K., Shinozaki O., Seto T. (2003). Size- dependent volatility of diesel nanoparticles: Chassis dynamometer experiments. Environ. Sci. Technol., 37, 1794- 1802.

Kwon S., & Hong J. (2010). Particle number and size distribution characteristics from diesel- and liquefied-natural-gas-fuelled buses for various emission certification modes in the Republic of Korea. Proc. IMechE 224 Part D: J. Automobile engineering, 1569-1579

Lähde T., Rönkkö T., Virtanen A., Schuck T. J., Pirjola L., Hämeri K., Kulmala M., Arnold F., Rothe D., & Keskinen J. (2009). Heavy-duty diesel engine exhaust aerosol particle and ion measurements. Environ. Sci. Technol., 43, 163-168.

Lähde T., Rönkkö T., Virtanen A., Solla A., Kytö M., Söderström C., & Keskinen J. (2010). Dependence between nonvolatile nucleation mode particle and soot number concentrations in an EGR equipped heavy-duty diesel engine exhaust. Environ. Sci. Technol., 44, 3175-3180

Lapuerta, M., Martos, F.J., & Herreros, J.M. (2007). Effect of engine operating conditions on the size of primary particles composing diesel soot agglomerates, J. Aerosol Sci., 38, 455-466.

Lee H., Myung C., & Park S. (2009). Time-resolved particle emission and size distribution characteristics during dynamic engine operation conditions with ethanol-blended fuels. Fuel, 88, 1680-1686

Lee K. O., Cole R., Sekar R., Choi M. Y., Kang J. S., Bae C. S., Shin H. D. (2003a). Morphological investigation of the microstructure, dimensions, and fractal geometry of diesel particulates. Proc. Combust. Inst., 29, 647-653.

Lee K. O., Cole, R., Sekar, R., Choi M. Y., Zhu J., Kang J., Bae C. (2001). Detailed characterization of morphology and dimensions of diesel particulates via thermophoretic sampling. SAE 2001-01-3572.

Lee K. O., Seong H., Sakai, S., Hageman, M., and Rothamer, D. (2013). Detailed morphological properties of nanoparticles from gasoline direct injection engine combustion of ethanol blends. SAE 2013-24-0185.

Lee K.O., Zhu J., Ciatti S., Choi M.Y. (2003b). Sizes, graphitic structure and fractal geometry of light-duty diesel engines particulates. SAE 2003-01-3169.

Lee, K.O., Cole, R., Sekar, R., Choi, M.Y., Kang, J.S., Bae, C.S., & Shin, H.D. (2002). Morphological Investigation of the Microstructure, Dimensions, and Fractal Geometry of Diesel Particulates. Proceedings of the Combustion Institute, 2002, 29, 647-653.

Lemmetty M., Vehkamäki H., Virtanen A., Kulmala M., & Keskinen J. (2007). Homogeneous ternary H2SO4–NH3–H2O nucleation and diesel exhaust: A classical approach. Aerosol and Air Quality Research, 7, 489–499.

Li N., Sioutas C., Cho A., Schmitz D., Misra C., Sempf J., Wang M., Oberley T., Froines J., & Nel A. (2003). Ultrafine particulate pollutants induce oxidative stress and mitochondrial damage. Environ. Health Perspect. 111, 455–460

Li T., Chen X., & Yan Z. (2013). Comparison of fine particles emissions of light-duty gasoline vehicles from chassis dynamometer tests and on-road measurements. Atmospheric Environment, 68, 82-91

Lim J., Lim C., & Yu L. (2009). Composition and size distribution of metals in diesel exhaust particulates. J. Environ Monit. 11, 1614-1621

Limbach L., Wick P., Manser P., Grass R., Bruinink A., & Stark W. (2007). Exposure of engineered nanoparticles to human lung epithelial cells: influence of chemical composition and catalytic activity on oxidative stress. Environ. Sci. Technol. 41, 4158-4163

Liu Z., Ge Y., Tan J., He C., Shah A., Ding Y., Yu L., & Zhao W. (2012). Impacts of continuously regenerating trap and particle oxidation catalyst on the NO2 and particulate emissions emitted from diesel engine. J. Environmental Sciences, 24, 624-631

Lovik M., Hogseth A., Gaarder P., Hagemann R., & Eide I. (1997). Diesel exhaust particles and carbon black have adjuvant activity on the local lymph node response and systemic IgE production to ovalbumin. Toxicology 121, 165–178

Mamakos A. Dardiotis C., Marotta A., Martini G., Manfredi U., Colombo R., Sculati M., Le Lijour P., & Lanappe G. (2011b). Particle emissions from a Euro 5a certified diesel passenger car, EUR 24855 EN.

Mamakos A., Carriero M., Bonnel P., Demircioglu H., Douglas K., Alessandrini S., Forni F., Montigny F., & Lesueur D. (2011a). EU-PEMS PM evaluation program – Second Report – Study on post DPF PM/PN emissions, EUR 24793.

Mamakos A., Dardiotis C., Martini G., & Krasenbrink A. (2011c). Assessment of particle number limits for petrol vehicles. EU report. http://circa.europa.eu/Public/irc/enterprise/automotive/library?l=/mveg_vehicle_emissions/107th_january_2011&vm=detailed&_sb=Title

Mamakos A., Martini G., & Krasenbrink A. (2012). Particle measurement programme. volatile particle remover calibration round robin. Report EUR 25512 EN

Mamakos A., Martini G., Manfredi U. (2013a). Assessment of the legislated particle number measure,ent procedure for a Euro 5 and Euro 6 compliant diesel passenger cars under regulated and unregulated conditions. J. Aerosol Sci. 55, 31-47

Mamakos A., Martini G., Marotta A., Manfredi U. (2013b). Assessment of different technical options in reducing particle emissions from gasoline direct injection vehicles. J. Aerosol Sci. 63, 115-125

Manke A., Wang L., & Rojanasakul Y. (2013). Mechanisms of nanoparticle-induced oxidative stress and toxicity. BioMed Research International, ID 942916, 15 pages

Maricq M. (2007). Chemical characterization of particulate emissions from diesel engines: a review. J. Aerosol Sci., 38, 1079-1118.

Maricq M. (2012). Soot formation in ethanol/gasoline fuel blend diffusion flames. Combustion and Flame, 159, 170-180

Maricq M., Chase R., Podsiadlik D., & Vogt R. (1999a). Vehicle exhaust particle size distributions: a comparison of tailpipe and dilution tunnel measurements. SAE 1999-01-1461.

Maricq M., Chase R., Xu N., & Laing P. (2002). The effects of the catalytic converter and fuel sulfur level on motor vehicle particulate matter emissions: light duty diesel vehicles, Environ. Sci. Technol. 36:283-289.

Maricq M., Munoz R., Yang J., & Anderson R. (2000). Sooting tendencies in an air-forced direct injection spark-ignition (DISI) engine. SAE 2000-01-0255.

Maricq M., Podsiadlik D., & Chase R. (1999b). Examination of the size-resolved and transient nature of motor vehicle particle emissions, Environ. Sci. Technol. 33:1618-1626.

Maricq M., Podsiadlik D., Brehob D., & Haghgooie M. (1999c). Particulate emissions from a direct-injection spark ingnition (DISI) engine. SAE 1999-01-1530.

Maricq M., Szente J., Loos M., & Vogt R. (2011). Motor vehicle PM emissions measurement at LEV III levels, SAE 2011-01-0623.

Markisz J., Pielecha J., & Gis W. (2009). Gaseous and particle emissions results from light duty vehicle with diesel particle filter. SAE 2009-01-2630

Mathis U., Kaegi R., Mohr M., Zenobi R. (2004b). TEM analysis of volatile nanoparticles from particle trap equipped diesel and direct-injection spark-ignition vehicles. Atmospheric Environment 38, 4347–4355

Mathis U., Mohr M., Kaegi R., Bertola A., & Boulouchos K. (2005). Influence of diesel engine combustion parameters on primary soot particle diameter. Environ. Sci. Technol., 39, 1887-1892

Mathis U., Mohr M., Ristimäki J., Keskinen J., Ntziachristos L., Samaras Z., & Mikkanen P. (2004a). Sampling conditions for the measurement of nucleation mode particles in the exhaust of a diesel vehicle. Aerosol Sci. Technol., 38, 1149-1160.

Matter, U. & Siegmann K. (1997). The influence of particle filter and fuel additives on turbo diesel engine exhaust. J. Aerosol Sci. 28, S1, 51-52

May J. (2011). Particulate emissions from typical light-duty vehicles taken from the European fleet equipped with a variety of emissions control technologies. 15th ETH conference on Combustion Generated Nanoparticles, June 26-29, Zürich, Switzerland.

May J., Bosteels D., Such C., Nicol A., & Andersson J. (2008). Heavy duty engine particulate emissions: application of PMP methodology to measure particle number and particulate mass, SAE 2008-01-1176.

Mayer A., Czerwinski J., Kasper M., Ulrich A., & Mooney J. (2012). Metal oxide particle emissions from diesel and petrol engines. SAE 2012-01-0841

Mayer A., Czerwinski J., Matter U., Wyser M., Scheidegger, Kieser D., & Weidhofer J. (1998). VERT: Diesel nano-particulate emissions: properties and reduction strategies. SAE 980539.

Mayer A., Ulrich A., Czerwinski J., & Mooney J. (2010). Metal-oxide particles in combustion engine exhaust. SAE 2010-01-0792.

Menon S., Hansen J., Nazarenko L., & Luo, Y. (2002). Climate effects of black carbon aerosols in China and India. Science 297, 2250-2253.

Merkisz J., Pielecha J., & Gis W. (2009). Gaseous and particle emissions results from light duty vehicle with diesel particle filter. SAE 2009-01-2630

Merola S., Vaglieco B.M., Zarinchang J. (2003). Simultaneous detection of NOx and particulate in exhaust of a CR diesel engine by UV- visible spectroscopy. SAE 2003- 01-0786.

Meyer N.K., & Ristovski Z.D (2007). Ternary Nucleation as a mechanism for the production of diesel nanoparticles: Experimental analysis of the volatile and hygroscopic properties of diesel exhaust using the volatilization and humidification tandem differential mobility analyzer. Environ. Sci. Technol., 41, 7309–7314.

Mohr M., Forss A., & Lehmann U. (2006). Particle emissions from diesel passenger cars equipped with a particle trap in comparison to other technologies, Environ. Sci. Technol. 40: 2375-2383.

Mohr M., Forss A., & Steffen D. (2000). Particulate emissions of gasoline vehicles and influence of the sampling procedure, SAE 2000-01-1137.

Mohr M., Lehmann U., & Margaria G. (2003a). ACEA programme on the emissions of fine particulates from passenger cars (2): Part 1: Particle characterisation of a wide range of engine technologies, SAE 2003-01-1889.

Mohr M., Lehmann U., & Margaria G., (2003b). ACEA programme on the emissions of fine particulates from passenger cars (2): Part 2: Effect of sampling conditions and fuel sulphur content on the particle emission, SAE 2003-01-1890.

Mordukhovich I., Wilker E., Suh H., Wright R., Sparrow D., Vokonas P., & Schwartz, J. (2009). Black carbon exposure, oxidative stress genes, and blood pressure in a repeated-measures study. Environ. Health Perspect. 117(11), 1767-1772

Myung C., Choi K., Kim J., Lim Y., Lee J., & Park S. (2012). Comparative study of regulated and unregulated toxic emissions characteristics from a spark ignition light-duty vehicle fueled with gasoline and liquid phase LPG (liquefied petroleum gas). Energy, 44, 189-196

Nash D., Baer T., & Johnston M. (2006). Aerosol mass spectrometry: an introductory review. Int. J. Mass Spectrometry, 258, 2-12.

Neer A., & Koylu U. (2006). Effect of operating conditions on the size, morphology, and concentration of submicrometer particulates emitted from a diesel engine. Combustion and Flame, 146, 142-154

Ng I. P., Ma H., & Kittelson D. (2007). Comparing measurements of carbon in diesel exhaust aerosols using the aethalometer, NIOSH method 5040, and SMPS. SAE 2007-01-0334

Ntziachristos L., Cho A., Froines J., Sioutas C. (2007). Relationship between redox activity and chemical speciation of size fractionated particulate matter. Part. Fibre Toxicol. 4, 5

Ntziachristos L., Giechaskiel B., Pistikopoulos P., & Samaras Z. (2005). Comparative assessment of two different sampling systems for particle emission type-approval measurements, SAE 2005-01-0198.

Ntziachristos L., Giechaskiel B., Pistikopoulos P., Fysikas E., Samaras Z. (2003). Particle emissions characteristics of different on-road vehicles. SAE 2003-01-1888

Ntziachristos L., Giechaskiel B., Pistikopoulos P., Samaras Z., Mathis U., Mohr M., Ristimäki J., Keskinen J., Mikkanen P., Casati R., Scheer V., Vogt R., (2004a). Performance evaluation of a novel sampling and measurement system for exhaust particle characterization. SAE 2004-01-1439.

Ntziachristos L., Mamakos A., Samaras Z., Mathis U., Mohr M., Thompson N., Stradling R., Forti L., & de Serves C. (2004b). Characterization of exhaust particulate emissions from road vehicles: results for light-duty vehicles, SAE 2004-01-1985.

Ntziachristos, L., Amanatidis, S., Giechaskiel, B., Samaras, Z., & Bergmann, A. (2013). Use of a catalytic stripper as an alternative to the original PMP measurement protocol. SAE 2013-01-1563.

Oberdörster G. (1996). Significance of particle parameters in the evaluation of exposure–dose relationships of inhaled particles. Inhalation Toxicology 8, 73–90

Oberdörster G. (2000). Toxicology of ultrafine particles: in vivo studies. Philosophical Transactions of the Royal Society Series A 258, 2719–2740

Oberdörster G., Sharp Z., Atudorei V., Elder A., Gelein R., Kreyling W., & Cox C. (2004). Translocation of inhaled ultrafine particles to the brain. Inhal Toxicol. 16(6-7), 437-45.

Okada S., Kweon C., Stetter J., Foster D., Shafer M., Christensen C., Schauer J., Schmidt A., Silverberg A., & Gross D. (2003). Measurement of trace metal composition in diesel engine particulate and its potential for determining oil consumption. SAE 2003-01-0076

Onasch T., Trimborn A., Fortner E., Jayne J., Kok G., Williams L., Davidovits P. & Worsnop D. (2012). Soot particle aerosol mass spectrometer: development, validation, and initial application. Aerosol Sci. Technol., 46, 804-817.

Pagels J., Khalizov A., McMurry P., & Zhang R. (2009). Processing of soot by controlled sulphuric acid and water condensation—mass and mobility relationship. Aerosol Sci. Technol., 43, 629-640.

Pandya R., Solomon G., Kinner A., & Balmes J.R. (2002). Diesel exhaust and asthma: Hypotheses and molecular mechanisms of action. Environmental Health Perspectives, 110, 103-112.

Park K., Cao F., Kittelson D. B., McMurry P. H. (2003). Relationship between particle mass and mobility for diesel exhaust particles. Environ. Sci. Technol., 37, 577-583.

Park K., Kittelson D., & McMurry P. (2004). Structural properties of diesel exhaust particles measured by transmission electron microscopy (TEM): relationships to particle mass and mobility. Aerosol Sci. Technol., 38, 881-889.

Piock W., Hoffmann G., Berndorfer A., Salemi P., & Fusshoeller B. (2011). Strategies towards meeting future particulate matter emission requirements in homogeneous gasoline direct injection engines. SAE 2011-01-1212.

PMP (2003) Report of the GRPE particle measurement programme (PMP) government sponsored work programmes, July 2003.

Pope C. III (2000). Epidemiology of fine particulate air pollution and human health: biologic mechanisms and who's at risk? Environ. Health Perspect. 108, 713–723

Price P., Stone R., Collier T., Davies M., & Scheer V. (2006). Dynamic particulate measurements from a DISI vehicle: a comparison of DMS500, ELPI, CPC and PASS, SAE 2006-01-1077.

Ramanathan V., & Carmichael G. (2008). Global and regional climate changes due to black carbon. Nature Geoscience 1, 221-227

Rönkkö T., Lähde T., Heikkilä J., Pirjola L., Bauschke U., Arnold F., Schlager H., Rothe D., Yli-Ojanpera J., and Keskinen J. (2013). Effects of gaseous sulphuric acid on diesel exhaust nanoparticle formation and characteristics. Environ. Sci. Technol., 47, 11882−11889

Rönkkö T., Virtanen A., Kannosto J., Keskinen J., Lappi M., & Pirjola L. (2007). Nucleation mode particles with a nonvolatile core in the exhaust of a heavy-duty diesel vehicle. Environ. Sci. Technol., 41, 6384-6389.

Sager T., & Castranova V. (2009). Surface area of particle administered versus mass in determining the pulmonary toxicity of ultrafine and fine carbon black: comparison to ultrafine titanium dioxide. Particle and Fibre Toxicology 6, 15

Saito C., Nakatani T., Miyairi Y., Yuuki K., Makino M., Kurachi H., Heuss W., Kuki T., Furuta Y., Kattouah P., & Vogt C. (2011). New particulate filter concept to reduce particle number emissions, SAE 2011-01-0814.

Sakurai H., Tobias H., Park K., Zarling D., Docherty K., Kittelson D., McMurry P., Ziemann P. (2003). On-line measurements of diesel nanoparticle composition and volatility. Atmospheric Environment 37, 1199-1210

Salvi S., Blomberg A., Rudell B., & Kelly F. (1999b). Acute inflammatory responses in the airways and peripheral blood after short-term exposure to diesel exhaust in healthy human volunteers. American Journal of Respiratory and Critical Care Medicine, 159, 702-709.

Salvi S., Frew A., & Holgate S. (1999a). Is diesel exhaust a cause for increasing allergies? Clinical & Experimental Allergy, 29, 4-8.

Seaton A., Tran L., Aitken R., & Donaldson K. (2009). Safety of nanomaterials interdisciplinary research centre nanoparticles, human health hazard and regulation. J. R. Soc. Interface. doi:10.1098/rsif.2009.0252.focus

Seinfeld J., & Pandis S. (1998). Atmospheric chemistry and physics: from air pollution to climate change. Wiley: New York.

Seinfeld J.,& Pandis S. (1998). Atmospheric chemistry and physics: from air pollution to climate change. Wiley: NewYork.

Sgro L., D'Anna A., & Minutolo P. (2011). Charge fraction distribution of nucleation mode particles: New insight on the particle formation mechanism. Combustion and Flame 158, 1418-1425

Shakhashiri B.Z. (1983). Chemical demonstrations. Madison: University of Wisconsin Press.

Shakhashiri, B.Z.(1983). Chemical Demonstrations. Madison:University of Wisconsin Press

Shi J. P., & Harrison R. M. (1999). Investigation of ultrafine particle formation during diesel exhaust dilution. Environ. Sci. Technol. 33, 3730-3736

Shi J.P., Mark D., Harrison R.M. (2000). Characterization of particles from a current technology heavy-duty diesel engine. Environ. Sci. Technol. 2000, 34, 748-755.

Silva P., & Prather K. (1997). On-line characterization of individual particles from automobile emissions. Environ. Sci. Technol., 31, 3074-3080.

Skillas G., Qian Z., Baltensperger U., Matter U., & Burtscher H. (2000). The Influence of Additives on the Size Disribution and Composition of Particles Produced by Diesel Engines. Combust. Sci. and Tech. 154, 259-273

Sodeman D., Toner S., & Prather K. (2005). Determination of single particle mass spectral signatures from light-duty vehicle emissions. Environ. Sci. Technol., 39, 4569-4580.

Stenitzer M. (2003). Nano particle formation in the exhaust of internal combustion engines. Technischen Universität Wien, Wien.

Swanson J., & Kittelson D. (2010). Evaluation of thermal denuder and catalytic stripper methods for solid particle measurements. J. Aerosol Sci., 41, 1113-1122.

Swanson J., Kittelson D., Giechaskiel B., Bergmann A., & Twigg M. (2013). A miniature catalytic stripper for particles less than 23 nm. SAE 2013-01-1570.

Swanson J., Kittelson D., Watts W., Gladis D., & Twigg M. (2009). Influence of storage and release on particle emissions from new and used CRTs. Atmospheric Environment, 43, 3998-4004.

Szybist J., Youngquist A., Barone T., Storey J., Moore W., Foster M., & Confer K. (2011). Ethanol blends and engine operating strategy effects on light-duty spark-ignition engine particle emissions. Energy & Fuels, 25 (11), 4977–4985

Tan P., Ruan S., Hu Z., Lou D., & Li H. (2014). Particle number emissions from light-duty diesel engine with viodiesle fuels under transient-state operating conditions. Applied Energy, 113, 22-31

Thompson N., Ntziachristos L., Samaras Z., Aakko P., Wass U., Hausberger S., & Sams T. (2004). Overview of the European "Particulates" project on the characterization of exhaust particulate emissions from road vehicles: results for heavy-duty engines, SAE 2004-01-1986.

Tobias H., Beving D., Ziemann P., Sakurai H., Zuk M., McMurry P., Zarling D., Waytulonis R., & Kittelson D., (2001). Chemical analysis of diesel engine nanoparticles using a Nano-DMA/thermal desorption particle beam mass spectrometer. Environ. Sci. Technol., 35, 2233-2243.

Toner S., Sodeman D., & Prathe, K. (2006). Single particle characterization of ultrafine and accumulation mode particles from heavy duty diesel vehicles using aerosol time-of-flight mass spectrometry. Environ. Sci. Technol., 40, 3912-3921.

Tzamkiozis T., Ntziachristos L., & Samaras Z. (2010). Diesel passenger car pm emissions: From Euro 1 to Euro 4 with particle filter, Atmospheric Environment 44:909-916.

Vaaraslahti K., Virtanen A., Ristimäki J., & Keskinen J. (2004). Nucleation mode formation in heavy-duty diesel exhaust with and without a particulate filter. Environ. Sci. Technol., 38, 4884-4890.

Virtanen A., Ristimäki J., Vaaraslahti K., & Keskinen J. (2004). Effect of engine load on diesel soot particles, Environ. Sci. Technol. 38:2551-2556.

Vogt R., Kirchner U., & Maricq M. (2006). Technical challenges with low level PM mass and number measurements. Cambridge Particle Meeting, May 22, 2006.

Vogt R., Kirchner U., & Maricq M. (2010). Investigation of EURO-5/6 level particle number emissions of European diesel light duty vehicles. 14th ETH Conference, Zürich, August 1-4th, 2010.

Vouitsis E., Ntziachristos L., & Samaras Z. (2004). Modeling of diesel exhaust aerosol during laboratory sampling. Atmospheric Environment, 39, 1335-1345.

Vouitsis E., Ntziachristos L., & Samaras Z. (2008). Theoretical investigation of the nucleation mode formation downstream of diesel after-treatment devices. Aerosol and Air Quality Research, 8, 37-53

Wal R. L. V., Tomasek A. J. Soot oxidation: Dependence upon initial nanostructure. Combust. Flame 2003, 134, 1-9.

Wang X., & McMurry P. (2006). An experimental study of nanoparticle focusing with aerodynamic lenses. Int. J. of Mass Spectrom. 258, 30-36.

Wang X., Caldow R., Sem G., Hama N., & Sakurai H. (2010). Evaluation of a condensation particle counter for vehicle emission measurement: experimental procedure and effects of calibration aerosol material. J. Aerosol Sci., 41, 306-318.

Wehner B., Philippin S., & Wiedensohler A. (2002). Design and calibration of a thermodenuder with an improved heating unit to measure the size-dependent volatile fraction of aerosol particles. J. Aerosol Sci., 33, 1087-1093.

Weingartner E., Burtscher H., & Baltensperger U. (1997). Hygroscopic properties of carbon and diesel soot particles. Atmospheric Environment, 31, 2311-2327.

Wentzel M., Gorzawski H., Naumann K. H., Saathoff H., Weinbruch S. (2003). Transmission electron microscopical and aerosol dynamical characterization of soot aerosols. J.AerosolSci., 34, 1347-1370.

Whitaker P., Karpus P., Ogris M., & Hollerer P. (2011). Measures to reduce particulate emissions from gasoline DI engines. SAE 2011-01-1219.

Yang H., Barger M., Castranova V., Ma J., Yang J., & Ma J. (1999). Effects of diesel exhaust particles (DEP), carbon black, and silica on macrophage responses to lipopolysaccharide: evidence of DEP suppression of macrophage activity. Journal of Toxicology and Environmental Health A 58, 261–278

Young L., Liou Y., Cheng M., Lu J., Yang H., Tsai Y., Wang L., Chen C., & Lai J. (2012). Effect of biodiesel, engine load and diesel particulate filter on non-volatile particle number size distributions in heavy-duty diesel engine exhaust. J. Hazardous Materials, 199-200, 282-289

Yu J.Z., Xu J., & Yang H. (2002). Charring characteristics of atmospheric organic particulate matter in thermal analysis. Environmental Science & Technology, 36, 754–761.

Yu J.Z., Xu,J., &Yang H. (2002). Charring characteristics of atmospheric organic particulate matter in thermal analysis. Environ. Sci. Technol. 36, 754–761.

Zhang S., McMahon W, Frodin B, Toutoundjian H., & Cruz M. (2010). Particulate emissions from California LEV ii certified gasoline direct injection vehicles. 20th CRC on-road vehicle emissions workshop, March 22-23, 2010, San Diego, California.

Zheng Z., Durbin T., Karavalakis G., Johnson K., Chaudhary A., Cocker III D., Herner J., Robertson W., Huai T., Ayala A., Kittelson D., & Jung H. (2012). Nature of sub-23-nm particles downstream of the European particle measurement programme (PMP)-compliant system: A real time perspective. Aerosol Sci. Technol. 46, 886-896

Zheng, Z., Johnson, K., Liu, Z., Durbin, T., Hu, S., Huai, T., Kittelson, D., & Jung, H. (2011). Investigation of solid particle number measurement: existence and nature of sub-23 nm particles under PMP methodology. J. Aerosol Sci., 42, 883-897.

# Annex A: Description of PN systems

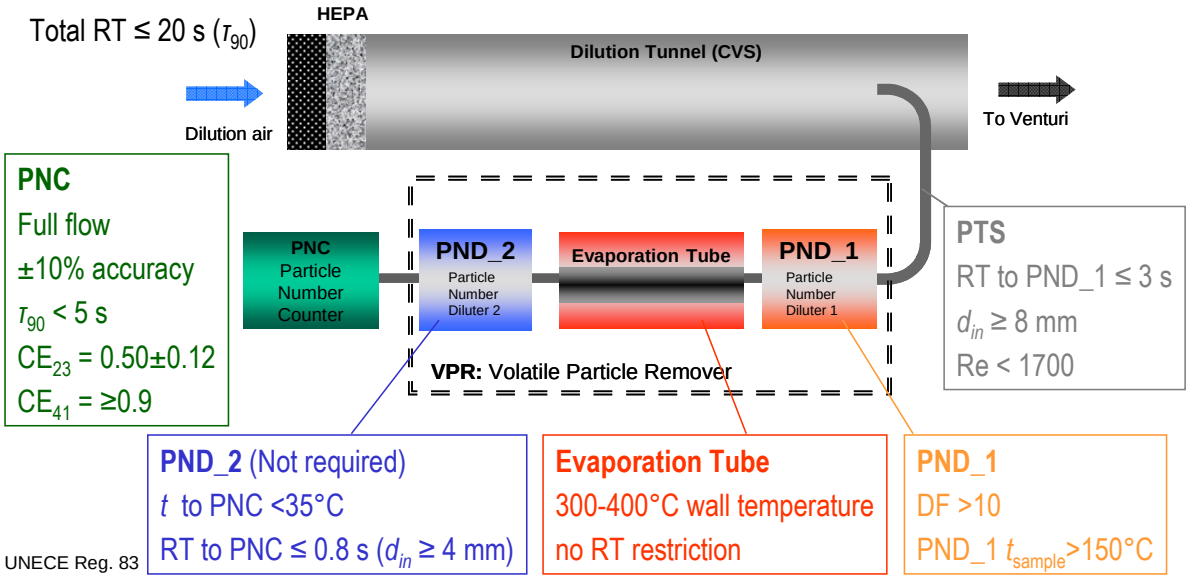


**Figure A1:** *According to UNECE Regulation 83, the Particle Number system should consist of a Volatile Particle Remover (VPR) and a Particle Number Counter (PNC). The VPR removes volatile particles and dilutes the sample. The PNC measures the number concentration of particles >23 nm to exclude possible confounding of measurements by low volatility hydrocarbons present as nucleation mode particles, while including the primary soot (spherule) size of 23 nm. The VPR should be connected to the full dilution tunnel (CVS) with a particle transfer tube (PTS) of inner diameter ≥8 mm (laminar flow). The residence time (RT) to the primary diluter (PND_1) of the VPR should be ≤3 s. The primary dilution factor (DF) should be ≥10 and the temperature of the diluted sample ≥150°C. In the VPR, after the PND_1, a heated tube with wall temperature between 300 and 400°C should exist. A secondary diluter (PND_2) is not required but the temperature at the inlet of the particle number counter (PNC) should be <35°C. The residence time from the VPR to the PNC should be ≤0.8 s and the diameter of the tube ≥4 mm. The PNC should be full flow (no internal splitting) with a response time of <5 s and counting efficiencies (CE) of 0.5±0.12 and >0.9 at 23 and 41 nm respectively. The slope should be 1±0.1. The total residence time in the VPR and PNC should be ≤20 s.*

## Annex B: Summary of studies that measured solid particles <23 nm.

The studies that measured solid particles <23 nm are summarized in Table B1. The following figures present some characteristic cases presented in the literature.

- Light-duty diesel vehicle (Figure B1)
- Heavy-duty diesel engine (Figure B2)
- G-DI engine (Figure B3)
- G-DI engine (Figure B4)
- Moped (artifact) (Figure B5)

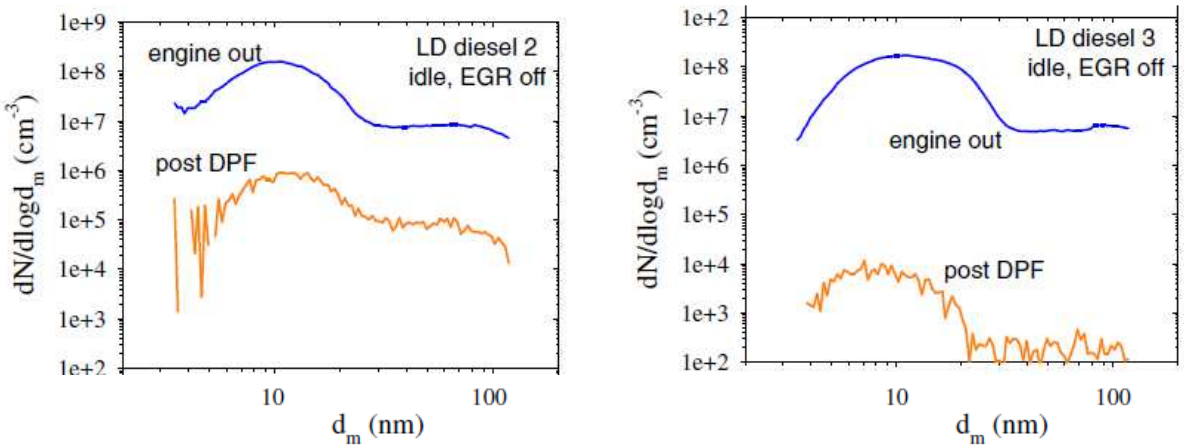


**Figure B1:** *Size distributions of two light-duty diesel vehicles (LD) engine out and post-DPF at idle (using an evaporation tube). From De Filippo and Maricq (2008).*

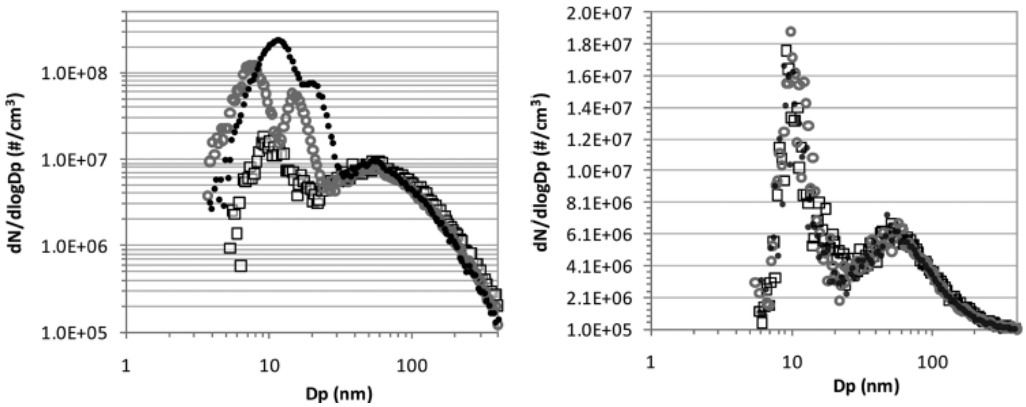


**Figure B2:** *Size distributions of a heavy-duty diesel engine without (left) and with (right) thermodenuder for different concentrations of gaseous sulfuric acid. Engine load 100%. From Rönkkö et al. (2013).*

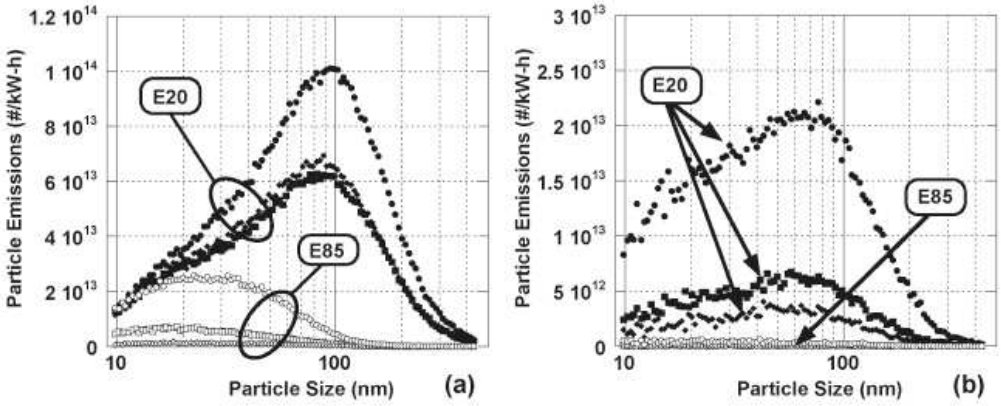


**Figure B3:** *Particle size distributions using the PMP method for E20 (closed symbols) and E85 (open symbols) for different operation modes for different injection timings (left and right panels) for a G-DI engine. From Szybist et al. (2011).*

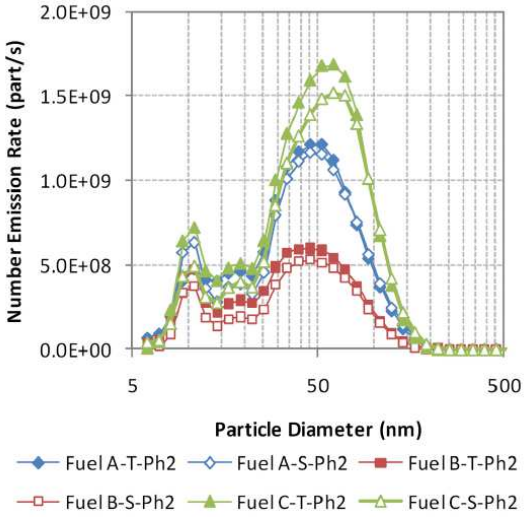


**Figure B4:** *Total (T) and Solid (S) particle number size distributions for three fuels. From Khalek et al. (2010).*

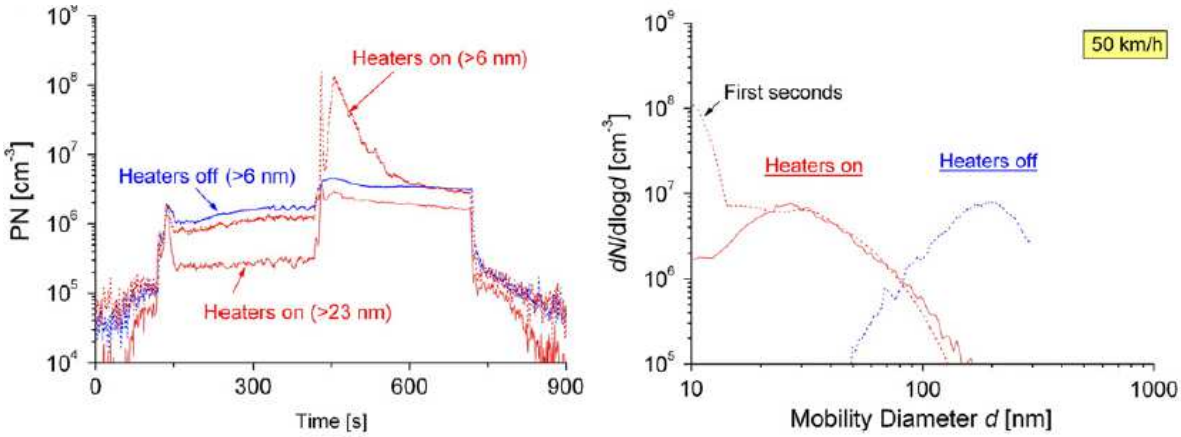


**Figure B4:** *Left panel: Particle number concentration during steady states of a moped (idle, 30 km/h, 50 km/h). Particle number size distribution for the 50 km/h. The increased concentration during the transition from 30 km/h to 50 km/h with the heaters on was an artifact of the PMP method due to re-nucleation. From Giechaskiel et al. (2010c).*

## Annex C: Uncertainties of the PN measurements

Although the PMP systems measure a concentration, the 'true' emissions are unknown due to the losses in the PN systems and the (unknown) inlet size distributions.
The penetration of a PN system (i.e. what percentage of the inlet particle concentration is measured) depends on the penetration of the VPR and the PNC (or counting efficiencies). The size-dependent VPR and PNC penetrations can vary from manufacturer to manufacturer, and in the case of the VPR can depend on the dilution conditions employed. The number concentration measured with each PN measurement system corresponds to the convolution of the size-dependent $PCRF_i$ and $CE_i$ and number concentration (size distribution), and therefore different implementation of the PMP methodology may result in different PN results. In order to improve the comparability of the different PMP systems, the regulations have introduced requirements for the VPR and PNC penetration curves. More specifically, the $PCRF_i$ of the VPR at 30 and 50 nm must be lower than 1.3 and 1.2 times that at 100 nm. The PNC must have a Counting Efficiency $CE_i$ of 0.5±0.12 at 23 nm and >0.9 at 41 nm and should also exhibit a 0.9 to 1.1 slope (i.e. 0.9 to 1.1 counting efficiency at a large size). Still though, systems complying with these requirements can exhibit differences especially when the Count Median Diameter (CMD) of the measured size distribution is close to 20 nm. However such a low CMDs has not been seen in modern European vehicles or heavy-duty engines running on standard reference fuels.

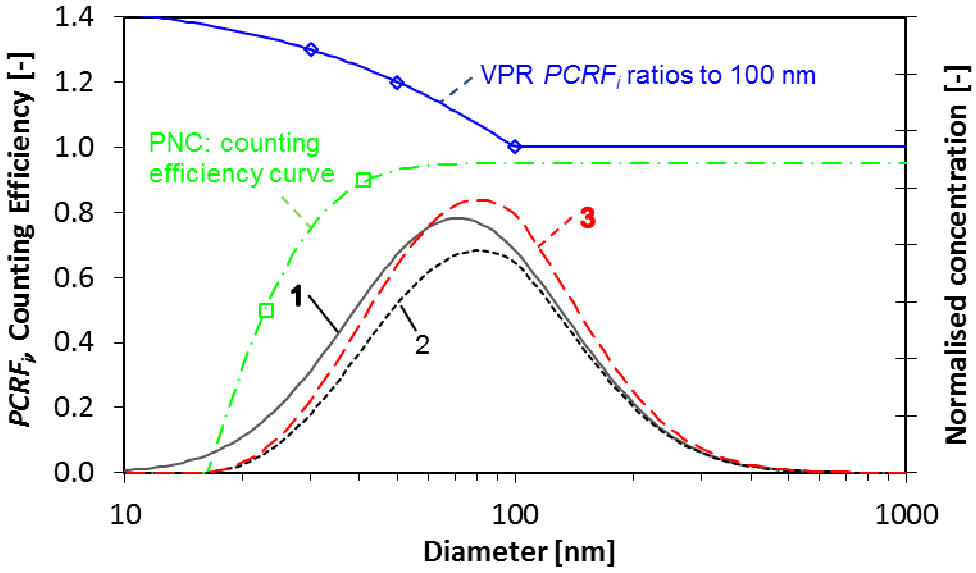


**Figure C1:** *Example showing size distributions at the inlet of the PN system inlet (1) and the final corrected based on the hypothetical PNC counting efficiency ($CE_i$) curve and the VPR $PCRF_i$ ratios at size i (3).*

Figure C1 shows a typical CE curve for a PNC ($CE_{23}$=0.5, $CE_{41}$=0.9, slope=0.95) and a VPR ($PCRF_{30}$=1.3x$PCRF_{100}$, $PCRF_{50}$=1.2x$PCRF_{100}$). A typical size distribution upstream of the PN system (VPR) with CMD 70 nm and standard deviation σ of 1.9 is also shown (see size distribution 1, assumed to be the 'true' emissions). Due to the penetration of the PN system (VPR and PNC), the measured size distribution by the PNC would be lower and shifted to the

right (see size distribution 2). Then a correction with the average PCRF of the VPR and the inverse of the slope of the PNC would be applied (x1.17/0.95 in this example). The final size distribution (and the PN concentration) (size distribution 3) would be different than the original size distribution (size distribution 1). For the specific example, the mode has been shifted 9 nm and the PN concentration is 1% less than the original 'true' PN concentration. Similarly with Figure C1, Table C1 gives the percentage (ratio) of the final PN result (corrected with the PNC slope and the VPR average PCRF) to the inlet 'true' concentration for different PNC counting efficiencies CE curves and different VPR $PCRF_i$ ratios that are legislation compliant. The three PNC cases (A, B, C) cover a very steep counting efficiency curve (case C: $CE_{23}$=0.62, $CE_{41}$=0.9, slope=0.9), a smooth (case B: $CE_{23}$=0.38, $CE_{41}$=0.9, slope=1.1) and an intermediate one (case A: $CE_{23}$=0.5, $CE_{41}$=0.9, slope=1.0). These cases seem extreme, but it should be taken into account that using different calibration material (i.e. phase, chemical composition, morphology) can result in big differences of the CEs. The differences in counting efficiencies between typical PNC calibration materials, emery oil and soot produced by a diffusion flame generator (mini CAST, Jing 2010) have been found to be ~0.15 and ~0.06 for 23 and 41 nm respectively (Giechaskiel and Bergmann 2011). The two $PCRF_i$ ratio cases (I, II) represent the worst case (case I: $PCRF_{30}$=1.3x$PCRF_{100}$, $PCRF_{50}$=1.2x$PCRF_{100}$) and an ideal case with no size dependent particle losses in the VPR (case II: $PCRF_{30}$=$PCRF_{50}$=$PCRF_{100}$).

**Table C1:** *Ratio of final PN result compared to the PN concentration at the inlet of the PN system for different inlet size distributions and PNC counting efficiencies $CE_i$ and VPR Particle Number Concentration Reduction Factor $PCRF_i$ ratios at size i.*

| | Case | A.I | A.II | B.I | B.II | C.I | C.II |
|---|---|---|---|---|---|---|---|
| PNC | $CE_{23}$ | 0.50 | 0.50 | 0.38 | 0.38 | 0.62 | 0.62 |
| | $CE_{41}$ | 0.90 | 0.90 | 0.90 | 0.90 | 0.90 | 0.90 |
| | slope | 1.00 | 1.00 | 1.10 | 1.10 | 0.90 | 0.90 |
| VPR | $PCRF_{30}$ | 1.3 | 1.0 | 1.3 | 1.0 | 1.3 | 1.0 |
| | $PCRF_{50}$ | 1.2 | 1.0 | 1.2 | 1.0 | 1.2 | 1.0 |
| CMD | σ | Final PN concentration compared to inlet concentration | | | | | |
| 10 | 1.3 | 1% | 1% | 0% | 0% | 0% | 0% |
| 20 | 1.4 | 33% | 37% | 23% | 26% | 34% | 38% |
| 30 | 1.6 | 61% | 65% | 53% | 56% | 69% | 74% |
| 40 | 1.7 | 77% | 79% | 70% | 71% | 84% | 86% |
| 50 | 1.8 | 87% | 85% | 81% | 80% | 92% | 91% |
| 70 | 1.9 | 98% | 92% | 95% | 89% | 102% | 96% |
| 90 | 2.0 | 104% | 95% | 102% | 93% | 106% | 98% |

For typical size distributions with medians between 50 and 90 nm the PN systems measure 80% up to 106% of the original 'true' emissions. The differences due to the different VPR $PCRF_i$ ratios are <9% (e.g. compare columns A.I&A.II, B.I&B.II, C.I&C.II), while those due to the different PNC counting efficiencies are <11% (e.g. compare columns A.I&B.I&C.I, A.II&B.II&C.II). The combination of the VPR and PNC can lead to up to 20% underestimation of the emissions; however, for typical penetrations and size distributions the underestimation is in the order of 5% (the average of columns A.I&A.II). However, in cases where the size distribution approaches the 50% cut-point of the PNC: 23 nm (e.g. 30 or 40 nm), the measured emissions can be only 60-70% of the inlet PN emissions (see rows with CMD 30 and 40 nm). Furthermore, different PN systems can exhibit up to 10% differences in the PN results, even if they comply with the legislation requirements, due to the different PNC and VPR penetrations (e.g. compare the values at each row).

Table C1 shows also that, if there is a nucleation mode, only a small percentage of it will be measured, which is positive if the nucleation mode is volatile, but negative if it is solid. For example, if the median of a volatile nucleation mode is 10 nm, then <1% of it will be measured, but if the median is 20 nm, then 23-38% of it will be measured. The contribution of these particles to the total PN result depends on the ratio of the nucleation and accumulation modes.

## Annex D: Experimental investigation of sub-23 nm particles nature

The following methods are some ideas for the investigation of sub-23 nm particles chemical composition. It should be realized however that high nanoparticle concentration or sampling times are needed to collect enough mass. Diffusion losses are also significant for such small particles and a correct sampling layout is very important.

**Transmission Electron Microscopy (TEM) and Energy Dispersive (X-ray) Spectroscopy (EDS):** Electron microscopy provides a means to examine the sizes and morphology of particles. This applies to solid particles; semi-volatile particles are difficult to detect because they evaporate under vacuum and heating by the electron beam. Image analysis provides a wealth of information about soot aggregates including: radius of gyration, size distribution of aggregates, fractal dimension, number of primary particles per aggregate, and size distribution of primary particles (Wentzel et al. 2003). The method has disadvantages as well. It is time consuming to analyze a sufficient number of particles to ensure statistical representatives. Also, care must be taken to interpret 3 dimensional shapes and sizes from the 2 dimensional images. Nevertheless, the projected area of diesel agglomerates is closely related to their mobility diameter (Park et al. 2004).

**Impactors and chemical analysis of filters:** In order to measure particles on the order of 30 nm and smaller, low pressure impactors are necessary. Quarz filters should be used. Details can be found in Okada et al. (2003), Ulrich and Wischser (2003), Lim et al. (2009). Traditional chemical analysis of motor vehicle exhaust PM is done by filter collection followed by solvent (e.g. dichloromethane) extraction and gas chromatography / mass spectrometry (GC/MS) analysis. This characterizes what is called the Soluble Organic Fraction (SOF). After the solvent is evaporated, SOF mass can be determined by weighing the residue. Usually, the solvent is partially evaporated to concentrate the SOF for GC/MS analysis for analysis of poly aromatic hydrocarbons (PAHs), nitro-PAHs, hopanes, steranes, and a long list of other compounds. Extraction with ethanol (or isopropanol) - water mixture can determine the sulfate content. Alternatively, it can be determined by ion chromatography. The filter can be weighed again and the difference to the original loaded filter gives the solid particle mass. Finally the residual solid can be analyzed by methods such as energy dispersive x-ray fluorescence (EDS) and inductively coupled plasma mass spectrometry (ICPMS) for elemental composition. Such comprehensive analyses are time consuming and expensive and, therefore, used primarily for research programs,

**Aerosol mass spectrometry:** Particle analysis by aerosol mass spectrometry is a field that has seen a lot of development in recent years (Johnston 2000, Nash et al. 2006, Maricq 2007, Bzdek et al. 2012). In this, either single particles are detected, sized, vaporized, and ionized, and the resulting ions are mass analyzed (Gard et al. 1997), or particles are collected onto a substrate under vacuum, heated to desorb semi-volatile species and ionized by electron impact (Jayne et al. 2000). The single particle approach has the advantages that it can in principle provide a complete chemical composition on a particle by particle basis. This allows one to distinguish internally and externally mixed aerosols. Its disadvantage is the difficulty in quantifying the composition, because the ionization efficiency is size and composition dependent. The

advantage of the second approach is that electron impact ionization allows the use of standard mass spectral databases to identify and quantify the chemical species. The disadvantage is that it detects only the semi-volatile species and the refractory components. The recent introduction of a laser based scheme is promising for vaporizing also the non-refractory components (Onasch et al. 2012).
These instruments detect with good efficiency particles larger than 100-200 nm. The lowest size of commercial instruments is about 30 nm in vacuum aerodynamic diameter. Modified aerodynamic lens systems have been used for laboratory-generated particles down to 3 nm (Wang and McMurry 2006). Today the most challenging part in ultrafine particle analysis is in determining the organic compounds. Over fragmentation by hard ionization causes losses of the original molecular information, while soft ionization is only sensitive to limited selective chemical groups. The presence of many similar and reactive organic compounds in particles also complicates the data interpretation. There are only a limited number of studies using the single particle analysis (Silva and Prather 1997, Toner et al. 2005; Sodeman et al. 2005) or thermal desorption / electron impact ionization (Tobias et al. 2001, Schneider et al. 2005, Giechaskiel et al. 2010c) to examine motor vehicle exhaust particles. The studies of metals are even less. See for example Okada et al. (2003) with Aerosol Time of Flight Mass Spectrometer (ATOFMS), Lee et al. (2006) with Single Particle Mass Spectrometery (SPMS) and Cross et al. (2012) with a Soot Particle Aerosol Spectrometer (SP-AMS). These techniques are usually combined with DMAs or SMPS to get size information in the <100 nm range; however <30 nm the transmission efficiency is very low.

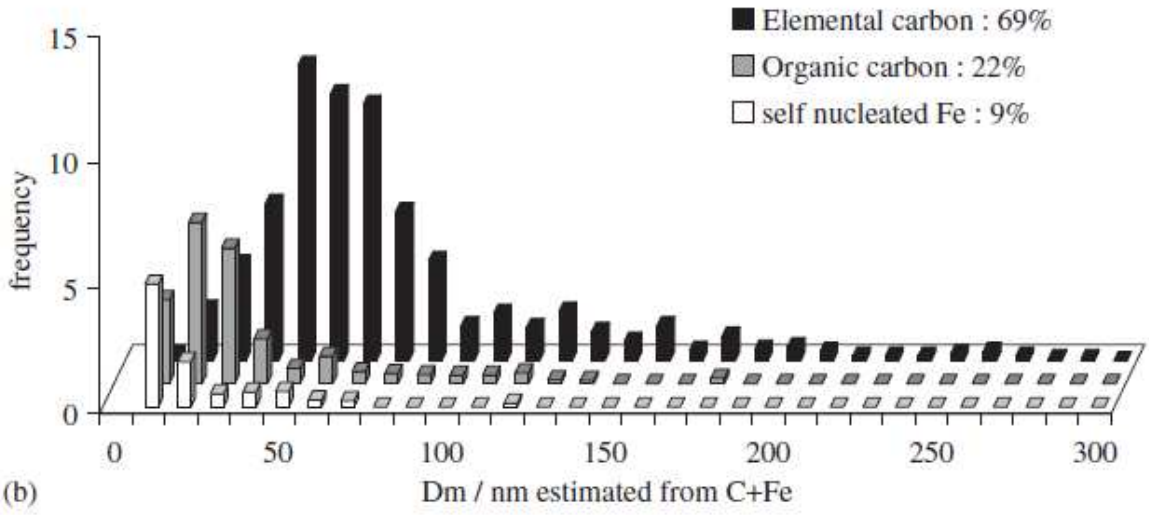


**Figure D1:** *Size distributions for three classes of diesel exhaust particles with high iron doping. Percent distributions refer to frequency of occurrence. From Lee et al. (2006).*

**Charge measurements:** It may be possible to distinguish engine formed from artifact formed solid particles by electrical charge. Particles formed by combustion are charged (bipolar) from ions formed chemically in flames. These attach to particles already during the flame and by the time combustion is complete there are essentially no free ions remaining. So particles formed subsequently, e.g., by nucleation, remain electrically neutral.

**Table B1:** *Summary of studies that measured solid particles <23 nm.*

| Authors | Publication | Technology | Cat. | Category | Characteristics | Aftertr. | Certif. | Fuel | Cycle | Diluter | Temp | Dilution | Instr. | Comments |
|---|---|---|---|---|---|---|---|---|---|---|---|---|---|---|
| Maricq et al. 1999c | SAE 1999-01-1530 | G-DI | LD | engine | 4 cyl., 1.83 L | none | | | Steady | EJ | 250C | 74x | SMPS | no separate NM, but peaks at 20 nm can exist |
| Maricq et al. 2000 | SAE 2000-01-0255 | G-DI | LD | engine | 1 cyl., 0.31 L | none | | | Steady | EJ | 200C | 64x | SMPS | NM at 30 nm at early spark timing |
| Khalek et al. 2010 | SAE 2010-01-2117 | G-DI | LD | vehicle | 2 L | TWC | LEV II | 3 - 80 ppm | various | PMP+CS | 350C | ? | EEPS | yes |
| Hedge et al. 2011 | SAE 2011-01-0636 | G-DI | LD | engine | 1.6 L with EGR | none | modern | <15 ppm ? | Steady | PMP+CS | 350C | 6x | EEPS | solid NM with high speed and EGR |
| Szybist et al. 2011 | Energy & Fuels, 25 (11), 4977–4985 | G-DI | LD | engine | 2 L | none | | <E85 | Steady | EJ+ET | 150C+350C | 5x6 | SMPS | yes, tail and means of 20-30nm in some cases |
| Johansson et al. 2013 | SAE 2013-24-0052 | G-DI | LD | cylinder | single cylinder | none | - | 1 ppm | Steady | FPS+TD | 350C | 24x | DMS | small tail but big part >23nm |
| Mamakos et al. 2013b | J. Aerosol Sci 63, 115-125 | G-DI | LD | vehicle | 2 L | TWC+(GPF) | Euro 5 | <10 ppm | various | PMP | 150C+350C | >25x5 | CPCs | yes, but possibly artifact |
| Mamakos et al. 2013b | J. Aerosol Sci 63, 115-125 | G-DI | LD | vehicle | 2 L Flexi Fuel | | | <10 ppm | various | PMP | 150C+350C | >25x5 | CPCs | yes, but possibly artifact |
| Mamakos et al. 2013b | J. Aerosol Sci 63, 115-125 | G-DI | LD | vehicle | 4.6 L, Dual | | Euro 4 | <10 ppm | various | PMP | 150C+350C | >25x5 | CPCs | yes, but possibly artifact |
| Ntziachristos et al. 2013 | SAE 2013-01-1563 | G-DI | LD | vehicle | 1.4 L | TWC | Euro 5 | <10 ppm | various | PMP or CS | 150C+350C | | SMPS | yes, below 10 nm at 120 km/h. CS could remove it |
| He et al. 2012 | Energy & Fuels, 26, 2014-2027 | G-DI | LD | engine | 1 cyl., 2 L | none | 2009 | | Steady | EJ | 130C | 5x2 | FMPS | yes, small NM |
| | | | | | | | | | | | | | | |
| Gidney et al. 2010 | Env. Sci. Techn. 44, 2562–2569 | P-FI | LD | vehicle | 4 cyl., 1.66 L MPI | TWC | 2000 | with additives | NEDC, steady | EJ+CS | 400C | 26x | DMS | yes, at 10 nm |
| Alger et al. 2010 | SAE 2010-01-0353 | P-FI | LD | engine | 2.4 L PFI with EGR | none | ? | ? | Steady | PMP+CS | 350C | ? | EEPS | sometimes small solid NM |
| Mayer et al. 2012 | SAE 2012-01-0841 | P-FI | LD | vehicle | 4 cyl., 2.165 L, MPI | TWC | 1985 | no metal additives | Steady | MD19+ET | 150C+300C | 100x | SMPS | yes, both idle and 50 km/h |
| Mayer et al. 2012 | SAE 2012-01-0841 | P-FI | LD | vehicle | 4 cyl., 1.997 L, MPI | TWC | 2008 | no metal additives | Steady | MD19+ET | 150C+300C | 100x | SMPS | no |
| Gupta et al. 2010 | Fuel, 89, 2230-2233 | P-FI | LD | engine | 4 cyl. | none | ? | ? | Steady | MD19 | ? | ? | EEPS | yes, at 10 nm or higher |
| Li et al. 2013 | Atm. Environ. 68, 82-91 | P-FI | LD | vehicle | 1.149 L | TWC ? | ? | ? | on-road | EJ | 180C | 8x | EEPS | yes, at 10 nm |
| Li et al. 2013 | Atm. Environ. 68, 82-91 | P-FI | LD | vehicle | 1.149 L | TWC ? | ? | ? | NEDC | EJ | 180C | 8x | EEPS | yes, at 10 nm |
| Huang et al. 2013 | Atm. Environ. 77, 703-710 | P-FI | LD | vehicle | 1.8 L | TWC | Euro 4 | <50 ppm | on-road | MD19 | 80C | 200x2.5 | EEPS | yes, size 10-20 nm |
| | | | | | | | | | | | | | | |
| Ntziachristos et al. 2003 | SAE 2003-01-1888 | 2 wheeler | | moped | 1 cyl., 0.05 L, carbu | oxi. Cat | 1999 | 125 ppm | Steady | Porous+TI | 250C | 12c | ELPI | yes |
| Ntziachristos et al. 2003 | SAE 2003-01-1888 | 2 wheeler | | Motorcycl | 1 cyl., 0.1 L, carbur | none | 1999 | 125 ppm | Steady | Porous+TI | 250C | 12c | ELPI | yes |
| Czerwinski et al. 2005 | 2005-01-1101 | 2 wheeler | | moped | 50 cm3, TSDI | Catalyst | 2002 | various | Steady | MD19 | 150C | ? | SMPS | yes, depending on the lube oil concentration |
| Czerwinski et al. 2006 | SAE 2006-01-1078 | 2 wheeler | | Scooter | carburator | Catalyst | 2004 | <1 ppm | Steady | MD19+ET | 150C+300C | | SMPS | yes, around 20 nm |
| Czerwinski et al. 2006 | SAE 2006-01-1078 | 2 wheeler | | Scooter | direct injection | Catalyst | 2002 | <1 ppm | Steady | MD19+ET | 150C+300C | | SMPS | yes, around 20 nm |
| Etissa et al. 2008 | Atm. Environ. 42, 183-195 | 2 wheeler | | Scooter | carburator | (oxi cat) | | | Steady | EJ+ET | 150C+400C | 64x | SMPS | yes, at 10 nm |
| Etissa et al. 2008 | Atm. Environ. 42, 183-195 | 2 wheeler | | Scooter | direct injection | (oxi cat) | | | Steady | EJ+ET | 150C+400C | 64x | SMPS | not clear |
| Giechaskiel et al. 2010c | Sci. Tot. Env. 408, 5106-5116 | 2 wheeler | | moped | direct injection | oxi cat | | 2% lube | Steady | EJ+ET | 150C+300C | 64x | SMPS | yes, around 25nm |
| Mayer et al. 2012 | SAE 2012-01-0841 | 2 wheeler | | Motorcycl | 2 cyl., 0.447 L, carbu | none | 1988 | no metal additives | Steady | MD19+ET | 150C+300C | 100x | SMPS | yes, both idle and 50 km/h |
| Mayer et al. 2012 | SAE 2012-01-0841 | 2 wheeler | | Scooter | 1 cyl., 0.124 L, port | Catalyst | 2008 | no metal additives | Steady | MD19+ET | 150C+300C | 100x | SMPS | yes, at 50 km/h |
| Czerwinski et al. 2013 | SAE 2013-24-0178 | 2 wheeler | | Scooter | 1 cyl., 0.049 L, | Catalyst | 2002 | | Steady | MD19+ET | 150C+300C | | SMPS | yes, probably lube not completely evaporated |
| Czerwinski et al. 2013 | SAE 2013-24-0178 | 2 wheeler | | Scooter | 1 cyl., 0.049 L, | Catalyst | 2004 | | Steady | MD19+ET | 150C+300C | | SMPS | yes, probably lube not completely evaporated |

| Authors | Publication | Technology | Cat. | Category | Characteristics | Aftertr. | Certif. | Fuel | Cycle | Diluter | Temp | Dilution | Instr. | Comments |
|---|---|---|---|---|---|---|---|---|---|---|---|---|---|---|
| Burtscher et al. 1998 | J. Aerosol Sci. 29, S2, 955-956 | Diesel | LD | engine | | | | | | | | | | Yes, with FBC |
| Skillas et al. 2000 | Comb Sci. Techn. 154, 259-273 | | | | | | | | | | | | | Yes, cerium |
| Kim and Choi 2008 | Renewable Energy, 33, 2222-2228 | Diesel | LD | engine | 2.5 L | Catalyst | | <30 ppm | Steady | EJ | 150C | 132 | SMPS | Yes, 20 nm at cold idle |
| De Filippo and Maricq 2008 | Env. Sci. Techn. 42, 7957-9962 | Diesel | LD | vehicle | 1.8 L, | DOC | 2003 | <50 ppm | Idle | EJ+TD | 200C+250C | 64 | SMPS | no solid NM |
| De Filippo and Maricq 2008 | Env. Sci. Techn. 42, 7957-9962 | Diesel | LD | vehicle | 2.7 L | DOC+SCR+D | 2007 | <25 ppm | Idle, <30 mph | EJ+ET | 200C+450C | 64 | SMPS | yes, when no EGR. 10 nm. No solid NM at speeds >4( |
| De Filippo and Maricq 2008 | Env. Sci. Techn. 42, 7957-9962 | Diesel | LD | vehicle | 6.7 L | DOC+LNT+D | 2007 | <25 ppm | Idle | EJ+ET | 200C+450C | 64 | SMPS | yes, when no EGR. 10 nm |
| Merkisz et al. 2009 | SAE 2009-01-2630 | Diesel | LD | vehicle | 4 cyl, 2 L | DOC+DPF | Euro 4 | <10 ppm | on-road | APC | 350C | ? | EEPS | yes, at accelerations |
| Dwyer et al. 2010a | J. Aerosol Sci. 41, 541-552 | Diesel | LD | vehicle | 4 cyl., 2 L | DOC+DPF | Euro 4 | <15 ppm | Regeneration | MD19+ET | 150C+300C | ? | CPC | Yes, during one EUDC (differnece of CPCs), with FBC |
| Dwyer et al. 2010b | Atm. Environ. 44, 3469-3476 | Diesel | LD | vehicle | 4 cyl., 2 L | DOC+DPF | Euro 4 | <15 ppm | NEDC | MD19+ET | 150C+300C | ? | CPC | No |
| Giechaskiel et al. 2010c | Sci. Tot. Env. 408, 5106-5116 | Diesel | LD | vehicle | | DOC | Euro 3 | <10 ppm | Steady | EJ+ET | 150C+300C | 64x | SMPS | yes, <10 nm but probably volatile |
| Mamakos et al. 2013a | J. Aerosol Sci 55, 31-47 | Diesel | LD | vehicle | 1.25 L | DOC+DPF | Euro 5 | <10 ppm | various | PMP | 150C+350C | >25x5 | CPCs | yes, at -7C, low EGR |
| Mamakos et al. 2013a | J. Aerosol Sci 55, 31-47 | Diesel | LD | vehicle | 2 L | DOC+DPF+S | Euro 6 | <10 ppm | various | PMP | 150C+350C | >25x5 | CPCs | yes, at motorway conditions, probably artifact |
| Armas et al. 2013 | SAE 2013-24-0176 | Diesel | LD | vehicle | 2 L | DOC+DPF | | | on-road | MD19+ET | 150C+300C | 17x6 | EEPS | yes, small tail, maybe noise |
| Cauda et al. 2006 | Env. Sci. Techn. 40, 5532-5537 | Diesel | LD | engine | 1 L, | DOC+DPF | ? | <10 ppm | Regeneration | EJ | 20C | 10-30x | SMPS | Yes, <20nm. Analysis showed carbon |
| Cauda et al. 2007 | Topics in Catalysis, 42-43, 253-257 | Diesel | LD | engine | 1 L, | DOC+DPF | ? | <10 ppm | Regeneration | EJ | 200C | 10-30x | SMPS | Yes, <20nm. Analysis showed carbon |
| Huang et al. 2013 | Atm. Environ. 77, 703-710 | Diesel | LD | vehicle | 1.9 L | DOC | Euro 3 | <50 ppm | on-road | MD19 | 80C | 200x2.5 | EEPS | small tail |
| Tan et al. 2014 | Applied Energy, 113, 22-31 | Diesel | LD | engine | 4 cyl, 3.3 L | none | - | 450 ppm + bio | Steady | MD19 | ? | 200x2.5 | EEPS | yes, around 10 nm |
| | | | | | | | | | | | | | | |
| Matter & Siegmann 1997 | J. Aerosol Sci. 28, S1, 51-52 | Diesel | HD | engine | | | | | Steady | | | | SMPS | Yes with additives |
| Mathis et al. 2005 | Env. Sci. Techn. 39, 1887-1892 | Diesel | HD | engine | 4 cyl., 6.64 L | none | | <15 ppm | Steady | EJ | 150C | 10x13 | SMPS | Yes at low engine load |
| Jung et al. 2005 | Comb Sci. Techn. 142, 276-288 | Diesel | HD | engine | 4 cyl., 4.5 L | none | 1999 | 300-500 ppm | Steady | EJ+CS | 300C | 27x31 | SMPS | Yes with additives around 10 nm |
| Kittelson et al. 2005 | J. Aerosol Sci. 36, 1089–1107 | Diesel | HD | engine | 6 cyl., 12 L | none | 1995 | <50 ppm | Steady | EJ+CS | 400C | 25x15 | SMPS | Yes at idle, 10 nm |
| Kittelson et al. 2006a | J. Aerosol Sci. 37, 913–930 | Diesel | HD | engine | 12 L | none | 1999 | <50 ppm | Steady | EJ+CS | 400C | 20x10 | SMPS | Yes at idle, 10 nm |
| Herner et al. 2007 | SAE 2007-01-1114 | Diesel | HD | vehicle | 8.3 L | CRT | 2000 | <15 ppm | various | MD19+ET | 150C+300C | 29x10 | CPC, E | yes, tail. Higher at idle |
| Rönkkö et al. 2007 | Env. Sci. Techn. 41, 6384-6389 | Diesel | HD | engine | 11.7 L | none | Euro IV | <10 ppm | Steady & On-r | Porous +T | 275C | 12x | SMPS | Yes, at speeds <40 km/h, size at 10 nm |
| Johnson et al. 2009 | Aerosol Sci. Techn. 43, 962-969 | Diesel | HD | vehicle | 6 cyl., 7.6 L | DPF | 1999 | <15 ppm | various | MD19+ET | 150C+300C | | CPCs | no solid NM |
| Johnson et al. 2009 | Aerosol Sci. Techn. 43, 962-969 | Diesel | HD | vehicle | 6 cyl., 14.6 L | CRT | 2000 | <15 ppm | on-road | MD19+ET | 150C+300C | | CPCs | yes, but below 10 nm |
| Giechaskiel et al. 2009 | SAE 2009-01-1767 | Diesel | HD | engine | | DOC+DPF | | <10 ppm | Regeneration | MD19+ET | 150C+300C | 100x | CPC | Yes, during passive regeneration |
| Lähde et al. 2009 | Env. Sci. Techn. 43, 163-168 | Diesel | HD | engine | 6 cyl., 10.6 L, EGR | none, DOC, | Euro IV | 36 ppm | Steady | Porous +T | 270C | 12x8 | SMPS | Yes, with none or DOC, 75% enine load |
| Lähde et al. 2010 | Env. Sci. Techn. 44, 3175-3180 | Diesel | HD | engine | 6 cyl., 10.6 L, EGR | none | Euro IV | <10 ppm | Steady | Porous +T | 265C | 12x8 | SMPS | Yes, at different loads, <10 nm |
| Mayer et al. 2010 | SAE 2010-01-0792 | Diesel | HD | engine | 4 cyl., 6.11 L | (DPF) | 1995 | <10 ppm | Steady | MD19+ET | 150C+300C | 100x | SMPS | yes at idle, or with FBC, reduced with DPF, <20 nm |
| Mayer et al. 2010 | SAE 2010-01-0792 | Diesel | HD | engine | 4 cyl., 6.36 L, EGR | (DPF) | 2005 | <10 ppm | Steady | MD19+ET | 150C+300C | 100x | SMPS | yes at idle, <20 nm, removed with DPF |
| Zheng et al. 2011 | J. Aerosol Sci. 42, 883-897 | Diesel | HD | vehicle | 6 cyl., 14.6 L | CRT | 2000 | <15 ppm | Steady | APC or CS | 150C+350C | 100x | variou | yes, mainly below 10 nm, probably artifa indication |
| Young et al. 2012 | J. Haz. Mater. 199-200, 282-289 | Diesel | HD | engine | 6 cyl, 6 L, no EGR | DOC+DPF | Euro I | <50 ppm | Steady | MD19+ET | 80C+300C | 15-300x | SMPS | yes, pre- and post DPF at 0% load |
| Armas et al. 2012 | Urban Climate, 2, 43-54 | Diesel | HD | vehicle | 6 cyl, 7.79 L, EGR | DOC+DPF | Euro III | 34 ppm + bio | on-road | MD19+ET | 80C+300C | 218x | EEPS | yes, at accelerations, at 10 nm |
| Zheng et al. 2012 | Aerosol Sci. Techn. 46, 886-896 | Diesel | HD | vehicle | 6 cyl., 14.6 L | CRT | 2000 | <15 ppm | on-road | MD19+ET | 150C+300C | 30x10 | variou | yes, mainly below 10 nm, probably artifact |
| Rönkkö et al. 2013 | Env. Sci. Techn. 47, 11882−11889 | Diesel | HD | engine | 6 cyl., 10.6 L, EGR | DOC+pDPF | Euro IV | 36 ppm | Steady | Porous +T | 265C | 12x8 | SMPS | Yes, at different loads, at 10 nm |
| Liu et al. 2012 | J. Env. Sciences, 24, 624-631 | Diesel | HD ? | engine | 4 cyl., 2 L | POC, CRDPF | ? | <50 ppm | Steady | EJ | 195C | 64 | ELPI | small tail |
| Huang et al. 2012 | J. Env. Sciences, 24, 1972-1978 | Diesel | HD | engine | 4 cyl, 5.3 L | none | Euro III | <50 ppm | Steady | MD19 | 80C | 200x2.5 | SMPS | yes, at 50% load or lower (not clear if really the ET w |
| Huang et al. 2012 | J. Env. Sciences, 24, 1972-1978 | Diesel | HD | vehicle | 4 cyl, 7.1 L | SCR | Euro IV | <50 ppm | Steady | MD19 | 80C | 200x2.5 | SMPS | yes, at 50% load or lower (not clear if really the ET w |
| Huang et al. 2013 | Atm. Environ. 77, 703-710 | Diesel | HD | vehicle | 7.1 L | SCR | Euro IV | <50 ppm | on-road | MD19 | 80C | 200x2.5 | EEPS | small tail |

European Commission
EUR xxxxx XX – Joint Research Centre – Institute for Energy and Transport

Title: Review on engine exhaust sub-23 nm particles

Author(s): B. Giechaskiel, G. Martini

Luxembourg: Publications Office of the European Union

2014 – 56 pp. – 21.0 x 29.7 cm

EUR – Scientific and Technical Research series – ISSN xxxx-xxxx (print), ISSN xxxx-xxxx (online)

ISBN xxx-xx-xx-xxxxx-x (PDF)
ISBN xxx-xx-xx-xxxxx-x (print)

doi:xx.xxxx/xxxxx

Abstract

In the current legislation particle number (PN) limits for solid particles >23 nm are prescribed. Target of this report was to investigate whether it is necessary and possible to measure <23 nm particles. In other words it was investigated: 1) whether smaller <23 nm solid particles are emitted from engines in considerable concentration focusing on Gasoline Direct Injection (G-DI) engines, 2) whether all volatile particles can be removed efficiently in the PN measurement systems 3) whether any artifacts happen in the PN systems (e.g. formation of non-volatile particles due to pyrolysis), and 4) whether by lowering the lower size the measurement uncertainty increases significantly.
The main conclusions are: 1) Engines emit solid sub-23 nm particles. The average percentage over a cycle (WLTP) is higher for G-DIs (<60%) compared to diesel engines (20%). These percentages are relatively low considering the emission limit levels (6x1011 p/km) and the repeatability (10-20%) and reproducibility of the method (50%). These percentages are close to the percentages expected theoretically not to be counted due to the 23 nm cut-off size (5-15%). High emissions can be found when additives are added in the fuel or lubricant. 2) The volatiles are not always removed efficiently in the PN measurement systems. The major issue is re-nucleation of sulfuric acid downstream of the evaporation tube. These particles typically do not grow at sizes above 23 nm. 3) There are indications of formation of 10 nm solid particles from hydrocarbons and sulfuric acid in the PN systems. 4) The measurement uncertainty due to differences between commercial systems will increase. It is estimated to be around 5% for measurements >10 nm, when no separate solid nucleation mode exists. 5) Based on the information today, the PN legislation should remain the same. However investigations should go on measuring <23 nm particles.

LB-NA-XXXXX-EN-N

## JRC Mission

As the Commission's in-house science service, the Joint Research Centre's mission is to provide EU policies with independent, evidence-based scientific and technical support throughout the whole policy cycle.

Working in close cooperation with policy Directorates-General, the JRC addresses key societal challenges while stimulating innovation through developing new methods, tools and standards, and sharing its know-how with the Member States, the scientific community and international partners.

*Serving society*
*Stimulating innovation*
*Supporting legislation*

Publications Office

ISBN xxx-xx-xx-xxxxx-